Pure Appl. Geophys.

DOI 10.1007/s00024-015-1069-y

Pure and Applied Geophysics

Earthquake Scenario-Based Tsunami Wave Heights in the Eastern Mediterranean and Connected Seas

Ocal Necmioglu[1] and Nurcan Meral Özel[1]

Abstract—We identified a set of tsunami scenario input parameters in a 0.5° × 0.5° uniformly gridded area in the Eastern Mediterranean, Aegean (both for shallow- and intermediate-depth earthquakes) and Black Seas (only shallow earthquakes) and calculated tsunami scenarios using the SWAN-Joint Research Centre (SWAN-JRC) code (Mader 2004; Annunziato 2007) with 2-arcmin resolution bathymetry data for the range of 6.5—Mw_{max} with an Mw increment of 0.1 at each grid in order to realize a comprehensive analysis of tsunami wave heights from earthquakes originating in the region. We defined characteristic earthquake source parameters from a compiled set of sources such as existing moment tensor catalogues and various reference studies, together with the Mw_{max} assigned in the literature, where possible. Results from 2,415 scenarios show that in the Eastern Mediterranean and its connected seas (Aegean and Black Sea), shallow earthquakes with $Mw \geq 6.5$ may result in coastal wave heights of 0.5 m, whereas the same wave height would be expected only from intermediate-depth earthquakes with $Mw \geq 7.0$. The distribution of maximum wave heights calculated indicate that tsunami wave heights up to 1 m could be expected in the northern Aegean, whereas in the Black Sea, Cyprus, Levantine coasts, northern Libya, eastern Sicily, southern Italy, and western Greece, up to 3-m wave height could be possible. Crete, the southern Aegean, and the area between northeast Libya and Alexandria (Egypt) is prone to maximum tsunami wave heights of >3 m. Considering that calculations are performed at a minimum bathymetry depth of 20 m, these wave heights may, according to Green's Law, be amplified by a factor of 2 at the coastline. The study can provide a basis for detailed tsunami hazard studies in the region.

Key words: Tsunami hazard, Eastern mediterranean, Aegean sea, Black sea.

1. Introduction

Tsunamis, as infrequent events, have the potential to cause massive loss of life and destruction of the infrastructure, including critical facilities, resulting in large economic losses that may require long recovery periods (Løvholt *et al*. 2012). The Indonesian tsunami led to the death of approximately 250,000 people, caused property and business damage totalling more than $4.4 billion, and left approximately 700,000 people homeless, leaving an unprecedented level of damage to the economy and infrastructure of the region (Ozel *et al*. 2011). The Tohoku event resulted in ~20,000 casualties and ~300,000 refugees with an economic cost of ~$122 billion. The critical damage at the Fukushima Daiichi Nuclear Power Plant resulted in severe releases of radioactivity, which resulted in serious concerns regarding long-term health and environmental hazards. According to the "Sendai Report—Managing Disaster Risks for a resilient future" published by the World Bank (2012), economic losses from disasters over the past 30 years are estimated at $3.5 trillion. The report "Lessons Learned From the Fukushima Nuclear Accident for Improving Safety of US Nuclear Plants" by a committee of the US National Research Council calls for nuclear plant licensees and regulators to continually look for new scientific information about nuclear plant hazards and methodologies for estimating their magnitudes, frequencies, and potential impacts and to incorporate new findings and methodologies as they become available. The report also emphasizes taking timely actions to implement countermeasures when new information results in substantial changes to the risk profiles at nuclear plants and also focuses on "beyond-design-basis events," which include low-frequency but high-magnitude "extreme" events—such as the earthquake and tsunami that damaged the Fukushima Daiichi plant on 11 March 2011 (Showstack 2014). Moreover, the Tohoku disaster showed that a long-term forecast should be based on only prehistoric paleoseismological data, and tsunami

[1] Kandilli Observatory and Earthquake Research Institute, Boğaziçi University, Istanbul, Turkey. E-mail: ocal.necmioglu@boun.edu.tr; ozeln@boun.edu.tr

Published online: 25 March 2015

hazard maps may need to be prepared for infrequent gigantic earthquakes as well as more frequent smaller-sized earthquakes (Satake 2011).

According to the available tsunami catalogues, tsunamis are most frequently generated by large submarine earthquakes ($\sim$75 % of the cases according to tsunami catalogues), and less frequently by volcanic activity and landslides ($\sim$5 and 10 %, respectively) and 10–15 % of the known tsunamis occurred in the Mediterranean (CIESM 2011). Despite the fact that 65 % of the referenced events in the historical catalogues should be considered as doubtful (Salamon *et al.* 2007) and a critical evaluation of these catalogues is a necessity (Ambraseys and Synolakis 2010), reliable sources of information, including catalog information with full confidence, paleotsunami and paleoseismology evidence still confirms the bitter truth: the Eastern Mediterranean and its connected seas (the Aegean, Marmara and Black Seas) are prone to tsunami hazard. Since the basins and sub-basins in the Eastern Mediterranean and its connected seas are small in comparison with large oceans, the challenges are greater than other parts of the world due to the short arrival times (less than 5–10 min) of the leading tsunami waves. With a fully developed infrastructure along the coast and with millions of tourists in the area, it is imperative that tsunami hazard needs are quantified. Tsunami scenarios are useful means for defining and evaluating tsunami hazards and constitute the primary step in tsunami risk mitigation and preparedness, potentially leading to defining the risk and, hence, contributing to sustainable coastal zone development (Tinti *et al.* 2005). As a preliminary step for possible tsunami hazard analysis in the the Eastern Mediterranean and its connected seas, we have attempted in our study to evaluate the distribution of tsunami wave heights from a set of earthquake sources for each source point of consideration in the range of Mw 6.5—Mw_{max} defined.

2. *Seismotectonic Setting of the Study Area*

The Black Sea Basin is composed of two main geological parts, namely the Western and Eastern, separated by the Mid Black Sea Ridge (Andrusov Ridge) that is formed from continental crust and overlain by sedimentary cover 5–6 km thick (Tari *et al.* 2000; Nikishin *et al.* 2003). The Western Black Sea Basin is underlain by oceanic to suboceanic crust and contains a sedimentary cover up to 19 km thick, whereas the Eastern Black Sea Basin is underlain by thinned continental crust approximately 10 km thick and up to 12 km of sediments (Nikishin *et al.* 2003). The rifting age has been suggested as the Aptian-Albian period (125–100.5 million years-Myr) for the entire Black Sea (Gorur 1997; Tari *et al.* 2000). The Black Sea began to close in the Eocene–Oligocene (56–23 Ma) time period following the closure of the Neotethys. Wheras the Eastern Black Sea has continued its closure from the Miocene up to the present (20–5 Myr), the central and western parts of the Black Sea have gone and undergo more complex neotectonics controlled by the by the northward motion of the African Plate, the western escape of the Anatolian block and Aegean extension, but with low-moderate seismic activity in the present times. Earthquakes took place on the borders of the deep-water basin, in general, with an average hypocentral depth of 5–20 km and a magnitude up to 6–8 mainly as a result of compressional stresses (Volvovsky 1989; Nikishin *et al.* 2003). This dominant compressional nature, as a result of the collision between the Eurasian and Arabian plates, has been verified by the stress fields obtained from the structural data such as thrusts in the Pontides and the Crimean part of the Black Sea, earthquake data such as Barka and Reilinger (1997) and Reilinger *et al.* (1997), stress field measurements in the Crimean and the Caucasus regions (Rastsvetaev 1987) and global positioning system (GPS) data (Barka and Reilinger 1997; Reilinger *et al.* 1997; Nikishin *et al.* 2003). GPS velocities indicate that there is a slight north–south shortening of the eastern half of the southern Black Sea coast, whereas a westward movement can be seen on the southwestern coast. The north–south motions in the Black Sea region are in the range of a few millimetres per year (mm/yr), in contrast to the velocities in the Anatolian region of $\sim$10–20 mm/yr. Geological and geophysical studies including offshore seismic reflection profiles, offshore morphology and recent seismicity indicates an active compressional tectonic regime in the Eastern Black

Sea region, which is also supported with the fault plane solution of studied events that took place in the last century (TARI *et al.* 2000). ALPTEKIN *et al.* (1986) provided the first evidence of active thrust faulting at the southern margin of the Black Sea in their analysis of the strongest instrumentally recorded 3 September 1968 Bartin earthquake to occur along the Black Sea margin in northwestern Turkey.

The history of the Eastern Mediterranean begins with the early Mesozoic breakup of Gondwana and is controlled by the collision of the African and Eurasian plates, the Arabian Eurasian convergence and current displacement of the Anatolian-Aegean microplates. The general agreement is that plate convergence takes place in this area (MCKENZIE 1970). A good summary of the development of tectonic research for the region together with main references on the tectonic processes and tectonic setting of the Eastern Mediterranean is given in ROBERTSON and MOUNTRAKIS 2006. The Eastern Mediterranean and the Levantine Basin are a remnant of the Mesozoic Neo-Tethys Ocean (ROBERTSON and DIXON 1984; STAMPFLI and BOREL 2002; GARFUNKEL 2004), where its northern arm is the Alpine chain between the African-Arabian and Eurasian plates as a result of convergence (BIJU-DUVAL *et al.* 1978). It accommodates important geomorphological features such as the Hellenic-Pliny-Strabo trenches, the Eastern Mediterranean Ridge, the Herodotus Basin, the Florence Rise and the Levantine Basin. A detailed discussion on the origin of the Eastern Mediterranean Basin is provided in various publications (GARFUNKEL 2004; AKSU *et al.* 2005). The Eastern Mediterranean region accommodates the Anatolia, Arabia, and Nubia plates and the Aegean microplate, which moves 30 ± 1 mm/yr to the southwest relative to Eurasia (EBELING *et al.* 2012; MCCLUSKY *et al.* 2000, 2003) and at a slightly lower velocity to the southwest relative to Nubia (EBELING *et al.* 2012; KREEMER and CHAMOT-ROOKE 2004; REILINGER *et al.* 2006). Aegean tectonics are characterized by 35–40 mm/yr north–south extension in central and southern Aegea (EBELING *et al.* 2012; KIRATZI and LOUVARI 2003; KIRATZI and PAPAZACHOS 1995; LE PICHON and ANGELIER 1979; MCCLUSKY *et al.* 2000; MCKENZIE 1978); east–west extension in the inner Hellenic Arc (EBELING *et al.* 2012; KREEMER and CHAMOT-ROOKE 2004; MCCLUSKY *et al.* 2003); and thrust faulting in the outer Hellenic Arc (EBELING *et al.* 2012; BENETATOS *et al.* 2004; MCKENZIE 1972, 1978). The western end of the Pliny and Strabo trenches lies southeast of Crete, however, their eastern ends are not well defined, but the broad deformation of the Pliny-Strabo zone has been correlated with the Burdur-Fethiye Fault Zone in southwestern Turkey (EBELING *et al.* 2012; HALL *et al.* 2009). GPS-derived velocity field data for the interaction zone of the Arabian, African (Nubian, Somalian), and Eurasian plates showes a counter-clockwise rotation of the Arabian plate, adjacent parts of the Zagros and central Iran, Turkey, and the Aegean/Peloponnesus at rates of 20–30 mm/yr occurring within the framework of the relatively slow moving (5 mm/yr) Eurasian, Nubian, and Somalian plates (REILINGER *et al.* 2006). On the basis of the observed kinematics, the deformation in the Africa-Arabia-Eurasia collision zone is driven in large part by rollback of the subducting African lithosphere beneath the Hellenic and Cyprus trenches aided by slab pull on the southeastern side of the subducting Arabian plate along the Makran subduction zone, and the separation of Arabia from Africa is a response to plate motions induced by active subduction (REILINGER *et al.* 2006). A fundamental discussion on the active tectonics of the Aegean Sea and surrounding regions is given in MCKENZIE (1978). The Aegean and its surroundings form the most active part of the Africa–Eurasia collision zone, responsible for the high level of seismicity in this region. It constitutes more than 60 % of the expected seismicity in Europe up to $Mw = 8.2$ (MORATTO *et al.* 2007; PAPAZACHOS 1990) as a result of the compressional motion between Europe and Africa and the resulting tectonic processes such as subduction of the eastern Mediterranean lithosphere under the Aegean along the Hellenic Arc and the westward motion of the Anatolian Block along the North Anatolia Fault (MORATTO *et al.* 2007; MCKENZIE 1970.) The whole Aegean Back Arc is mainly represented by normal faults (MORATTO *et al.* 2007; MCKENZIE 1978), whereas the dense shallow seismicity with low-angle thrust faults occurs along the Hellenic Arc (MORATTO *et al.* 2007; PAPAZACHOS 1990).

The tectonic setting of the Aegean and Eastern Mediterranean is complex; so is the associated discussion. Several other sources of information used in this study are related to studies focusing on fault classification and seismic zonation. A zonation for seismogenic sources of intermediate-depth earthquakes in the southern Aegean area is given by Papazachos and Papaioannou (1993). The maximum expected ground motion in Greece using a deterministic seismic hazard analysis based on an homogeneous earthquake catalog for the period of 426 BC–2003 applied on a seismogenic source model with representative focal mechanisms and a set of velocity models after applying a smoothing algorithm to the main shocks in the catalogue have been estimated by Moratto *et al.* (2007). Papaioannou and Papazachos (2000) provide a map of shallow earthquake sources based on previous work on seismic zonation in the Aegean and surrounding area, active tectonics and geological and geomorphological information. Maximum credible earthquake magnitudes (in the range 6.7–7.6 Mw) in the Aegean area constrained by tectonic moment release rates based on zonation corresponding to recent determinations of deformation rates from satellite data through the use of a merged historical and an instrumental earthquake catalog for the Aegean is provided by Koravos *et al.* (2003). A fault classification for the Aegean region is provided in Sboras *et al.* (2011). Caputo *et al.* (2012) provides a repository of geological, tectonic and active-fault data for Northern Greece and the Northern Aegean Sea based on a collection of all available published and unpublished historical and instrumental seismicity data supported by seismogenic sources recognized on the basis of geological, structural, morphotectonic, paleo-seismological and geophysical investigations, which was followed by critical examination of all collected data with the aim of identifiying as many as possible seismogenic source as possible, as well as the parameters and the characateristics associated. Both Sboras *et al.* (2011) and Caputo *et al.* (2012) are part of the SHARE Project (Basili *et al.* 2013). Mitsakaki *et al.* (2013) provide geometric characteristics of selected tectonic segments in the Hellenic Arc and Northern Aegean. A full description of the complexity of the seismotectonic setting of the study area is beyond the scope of this study and it has been addressed in many aspects by many studies, such as Bayrak and Bayrak 2011; Ben Avraham *et al.* 2008; Bohnhoff *et al.* 2005; Delibasis *et al.* 1999; Dewey *et al.* 1973; Eyidoğan and Jackson 1985; Ganas and Parsons 2009; Hatzfeld *et al.* 1993; Heuret *et al.* 2011; Howe and Bird 2010; Hyndman *et al.* 1997; Jolivet *et al.* 2013; Jost *et al.* 2002; Karabulut *et al.* 2006; Meier *et al.* 2007; Papadimitriou and Karakostas 2008; Papazachos *et al.* 1991; Papazachos 1996; Papazachos and Papaioannou, 1999; Pilidou *et al.* 2004; Reilinger *et al.* 2010; Saleh 2013; Saatçılar *et al.* 1999; Salamon *et al.* 2003; Scholz 1998; Shaw and Jackson 2010; Snopek *et al.* 2007; Stern 2002; Şengör *et al.* 1985; Strobl *et al.* 2014; Taymaz *et al.* 1990, 1991; Vannucci and Gasperini 2004; Yolsal-Çevikbilen and Taymaz 2012.

3. An Overview of Previous Tsunami Hazard Research in the Study Area

In addition to the earthquake and moment tensor catalogues and various individual references on earthquakes and seismic hazard analysis in the study region, information from studies specifically targeting tectonic tsunami hazard has also been added to the compiled database.

3.1. Black Sea

Dotsenko and Ingerov (2007) revised the quantitative characteristics of four historical events in the Black Sea based on spectral analysis of the digitized mareograms. They concluded that while the maximum heights of the recorded tsunami wave tide-gauge locations do not exceed 52 cm, an increase in the wave height with an increase in the magnitude is observed, as expected. They also reported that the typical periods of tsunami waves lie within the interval of 8–39 min (Dotsenko and Ingerov 2007).

In their tsunami modeling study for the Black Sea, Dotsenko and Ingerov (2010) concluded that the highest waves are formed at the coastal sites closest to the seismic source. They simulated mareogram records at 27 locations in the northern part of the

Black Sea based on 24 possible source zones and concluded that the maximum wave height should not exceed 3 m at any site while, for most of the sites, it is reasonable to expect a maximum of 1.5 m for $M = 7$.

3.2. Eastern Mediterranean and Aegean

A review of the terrestrial geologic records of the Aegean region showing that little geologic evidence has been identified for a many tsunamis reported in the catalogues was provided in Dominey-Howes (2006). In an attempt to develop some simple scenarios of earthquake-generated tsunamis in the Mediterranean, Tinti *et al.* (2005) identified four different seismogenic areas in the western, central and eastern sections of the basin and defined a seismic fault capable of generating an earthquake with a magnitude equal or larger than the highest magnitude registered throughout history.

Altinok *et al.* (2005) studied the 1881 Chios-Cesme (Mw 6.5) and 1949 Chios-Karaburun (Mw 6.7) earthquakes where associated earthquakes and co-seismic underwater failure-originated tsunamis affected Chios Island and Cesme. Salamon *et al.* (2007) collected and investigated ancient and modern tsunami reports in the Eastern Mediterranean to understand and model the typical tsunamigenic sources with possible characterization of the tsunami hazard along the Levant coasts. Their analysis indicated that only 35 % of the tsunami reports could be traced back to primary sources. In addition to critical compilation and assessment of the tsunami reports, they also modeled three typical scenarios and examined the more likely severe magnitudes, which leads toward the upper range of expected run-ups. They concluded that an offshore slump produced by a strong Dead Sea transform system earthquake may lead to 4- to 6-m run-up flooding the Syrian, Lebanese, and Israeli coasts, whereas tsunamis from remote earthquakes produce only 1- to 3-m run-ups in these coasts, but are more regional in extent. Yolsal *et al.* (2007) attempted to synthesize historical tsunamis and tsunami propagation in the Eastern Mediterranean Sea region, focusing specifically to the Hellenic and the Cyprus arcs and the Levantine Basin, and provided focal mechanism parameters for the 11 May 1222 Paphos and 8 August 1303 Crete earthquakes while at the same time providing their interpretation of tsunami source zones in the Eastern Mediterranean and Aegean Seas.

In their study, Lorito *et al.* (2008) selected three potential source zones located at short, intermediate and large distances from Southern Italy to study the impact of a large set of tsunamis resulting from earthquakes generated by major fault zones of the Mediterranean Sea. They argued that only a systematic identification of all possible sources along with their correlative tsunami scenarios is needed to deal with the uncertain source-impact zones and there is a need for considering both distant and local sources.

Okal *et al.* (2009) conducted a study on the 1956 Amorgos earthquake based on a normal mechanism fault with a rupture area of 75×40 km derived from the systematic relocation of the main shock and 34 associated events expressing extensional tectonics in the Hellenic subduction zone back-arc. Also supported with eye-witness reports, they argued that the observed tsunami is incompatible with a seismic dislocation source only and demonstrated this through hydrodynamic simulations using both the dislocation and landslide source models. This conclusion has been somehow further supported by Beisel *et al.* (2009) based on the spectral analysis of the tide-gauge record in the port of Yafo (Israel), as the coseismic tsunami source failed to capture significant spectral energy components while simulations resulted in tsunami waves with their heights close to that obtained from the record measured at Yafo. In fact, Beisel *et al.* (2009) succeeded in obtaining harmonics with frequencies very close to those measured at the tide gauge station when landslide movement, triggered by the main shock and/or by the largest aftershock, is suggested as a source of these tsunami waves.

Basili *et al.* (2013) states that while tsunamis generated by Mw = 8 earthquakes affect the entire basin, the impact of tsunamis generated by Mw = 7 earthquakes should be expected to be strong at many localities and conclude that a set of scenarios with regard to the epistemic uncertainties in the parametric fault characterization in terms of geometry, kinematics, and assessment of activity rates should be considered in tsunami hazard analysis.

Ebeling *et al.* (2012) reassessed four large (M ∼ 7) historical earthquakes occurring in various regions of the Hellenic Arc (on 6 October 1947, in the Peloponnesus; 9 February 1948, near Karpathos; and a couplet east of Rhodos on 24 and 25 April 1957), where the first two are associated with the damaging near-field tsunamis involving submarine slumping. A systematic assessment of the earthquake-generated tsunami hazard for Rhodes Island in the SE Aegean Sea based on several hypothetical, credible, near-field 'worst case' scenarios associated with seismic events of magnitude 8.0–8.4 has been presented in Mitsouidis *et al.* (2012).

Sørensen *et al.* (2012) provided the first probabilistic estimate of earthquake-generated tsunami hazard for the entire Mediterranean Sea based on deterministic tsunami wave propagation scenarios corresponding to earthquake activity rates estimated from the observed seismicity. Their results indicated that while the highest hazard in the eastern Mediterranean is due to the earthquakes along the Hellenic Arc, in fact most of the Mediterranean coastline is prone to tsunami impact, the probability of a tsunami wave exceeding 1 m somewhere in the Mediterranean in the next 30 years is close to 100 % (Sørensen *et al.* 2012). Their source model consists of 21 homogeneous zones chosen to be small enough to represent regions of relatively homogeneous earthquake activity while at the same time sufficiently large enough allowing for a stable statistical analysis of the source zone characteristics. However, the sizes of the zone areas they determined would not allow capturing the complexity of the seismo-tectonic setting presented in Fig. 1 in our view.

Yolsal-Çevikbilen and Taymaz (2012) numerically simulated the major and well-known earthquake-induced Eastern Mediterranean tsunamis of 365, 1222, 1303, 1481, 1494, 1822 and 1948 and proposed several hypothetical tsunami scenarios to demonstrate the characteristics of tsunami waves, propagations and effects of coastal topography. While they argue that the Cyprus Island acts as a natural barrier for tsunami waves in case of earthquakes along the Hellenic Arc, the Cyprus Arc and/or the Levantine Basin, they also emphasized the need for better geophysical, seismological and geological observations in the future for the improvement of tsunami simulations.

In their PTHA study, Løvholt *et al.* (2012) argued that in the Hellenic Arc, at the southern parts of Peloponnese and Crete, the run-up height for a return period of 500 years might well exceed 10 m.

A map of tsunamigenic zones in the Mediterranean region and its connected seas, including the Marmara Sea, the Black Sea and the SW Iberian Margin in the NE Atlantic Ocean, is provided in Papadopoulos *et al.* (2014) based on combined analysis of various sources such as historical documents, onshore and offshore geological signatures, geomorphological imprints, observations from selected coastal archeological sites, as well as instrumental records, eyewitnesses accounts and pictorial material concerning both seismic and non-seismic origins with a variable tsunamigenic potential.

Various other studies such as Papazachos *et al.* (1986), Soloviev (1990), Ranguelov and Gospodinov (1994), Dotsenko and Konovalov (1996), Yalçiner *et al.* (2004), Papadopoulos *et al.* (2011a, b), Pararas-Carayannis (2011), Mitsoudis *et al.* (2012) provide information on the tsunamis observed and/or analysed in the Black Sea, the Aegean Sea and the Eastern Mediterranean. All of these studies, whether presented here or not (except Sørensen *et al.* 2012), provide conclusions based on one or several selected earthquake-triggered tsunami scenarios. In this study, we have attempted to go beyond all of theses previous studies by not only considering all of the possible tsunamigenic earthquake sources but also considering their possible magnitude ranges.

4. *Parameterization of Tsunamigenic Earthquake Sources and Creation of the Tsunami Scenario Database*

Uncertainties in earthquake source parameters, such as strike, dip, rake and depth, and the effect of their variability on tsunami wave propagation and calculated wave heights at offshore coastal locations was discussed in Necmioğlu and Özel (2014). Among the various sources used to assign characteristics of

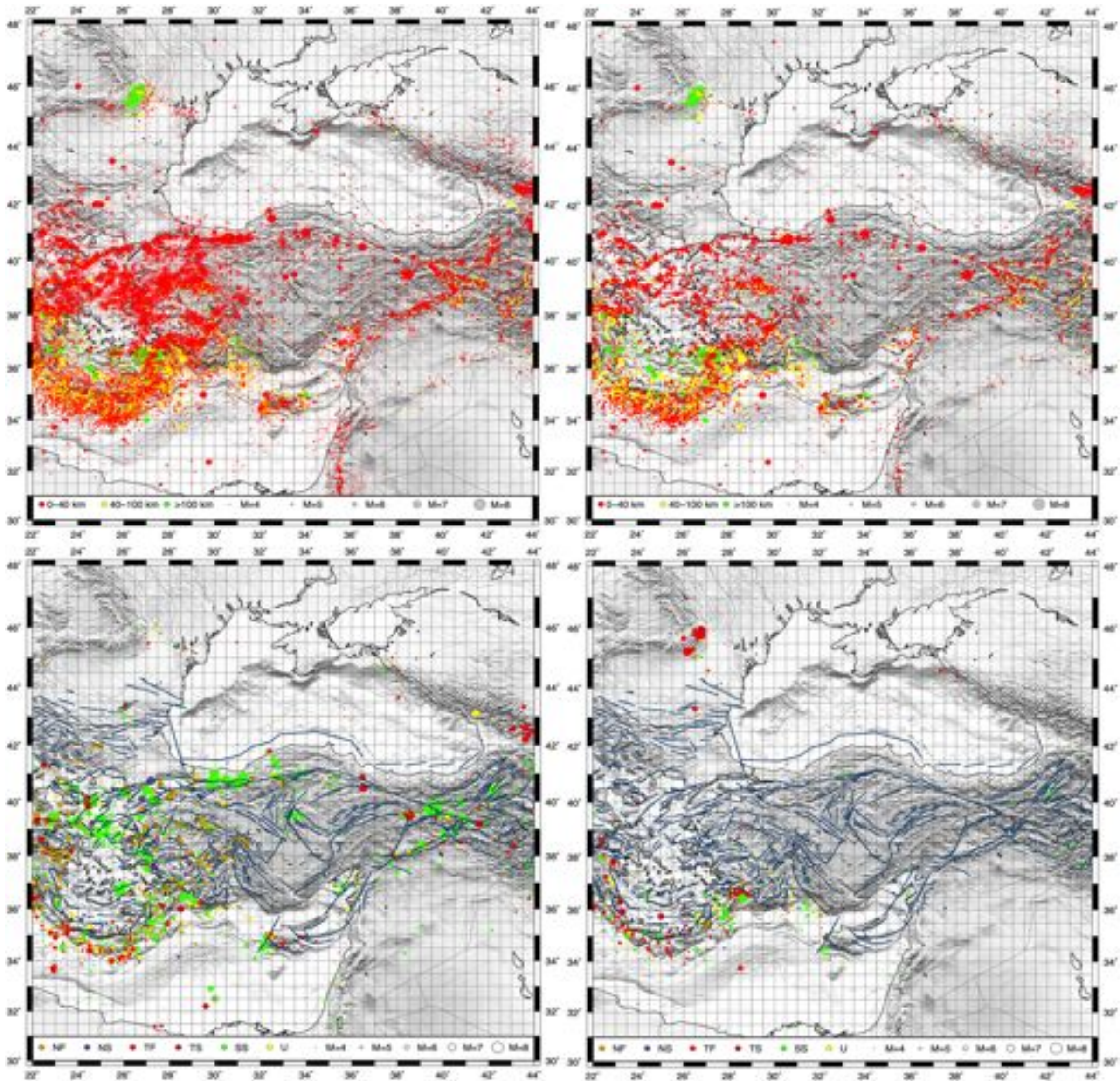

Figure 1
Consolidated seismicity maps from the International Seismological Centre (ISC), the Earthquake Mechanisms of the Mediterranean Area (EMMA; Vannucci and Gasperini 2004) and Kalafat *et al.* (2009) catalogs with no magnitude restriction (*upper left*) and with M > 4 (*upper right*). Fault types in the Eastern Mediterranean, Aegean and Black Seas according to Zoback (1992) derived from ISC, EMMA and Kalafat *et al.* (2009) moment tensor catalogs for the depth range of 0-40 km (*bottom left*) and 40–100 km (bottom right). *NF* normal faulting, *NS* normal faulting combined with considerable strike-slip component, *TF* thrust faulting, *TS* thrust faulting combined with considerable strike-slip component, *SS* strike-slip faulting, *U* unclassified type of faulting. Fault lines are taken from Basili *et al.* (2013). Figure modified from Necmioğlu and Özel (2014)

earthquake sources at each source point in this study, the first and main source was the available moment tensor catalogues (ISC Focal Mechanism Database; Vannucci and Gasperini 2004; Kalafat *et al.* 2009). The seismicity maps from ISC, EMMA and Kalafat *et al.* (2009) catalogues are given in Fig. 1. The events selected from the Reviewed ISC Bulletin focal mechanism database, which also includes important datasets such as the Global Centroid Moment Tensor (GCMT) Project, has a total of 466 events with

M ≥ 4.0 defined strike/dip/rake values out of 4,233 events for the range of 1 January 1911–1 January 2011 in the study area (30°–48°N/22°–44°E). The second release of the EMMA database (Vannucci and Gasperini 2004) is a very detailed and comprehensive compilation of earthquake source parameters. A total of 735 events from the EMMA catalog were considered in this study; 827 events with M ≥ 4.0 can be found in Kalafat *et al.* (2009), where earthquake source parameters of 46 % of the events included are originally calculated for that study; the rest were complied from other sources. Interpretation of the fault mechanism based on different moment tensor catalogues may lead to different conclusions. On the other hand, when combined, the catalogues may be used to identify zones with similar properties, as shown in Fig. 1. Seismicity maps shown in Fig. 1 helped to identify the locations of 0.5° × 0.5° bins at 0–40 and 40–100 km depth layers to be used in the source characterization and corresponding tsunami scenario creation (Fig. 2). The reason for considering two depth layers was to study the generation of tsunamis by intermediate-depth sources as suggested by Necmioğlu and Özel (2014). The variation of strike, dip and rake values through polar plots have been evaluated subjectively at 312 0.5° × 0.5° uniformly gridded bins for a 0–40 km shallow depth layer and 92 bins for a 40–100 km intermediate-depth layer in order to determine the dominant strike/dip/rake parameters in each bin. An additional database was the European Database of Seismogenic Faults (EDSF) compiled in the framework of the EU Seismic Hazard Harmonization in Europe (SHARE) Project (Basili *et al.* 2013; Sboras *et al.* 2011), which includes only faults that are deemed to be capable of generating earthquakes of magnitude equal to or larger than 5.5 with the aims at ensuring an homogenous input for use in ground-shaking hazard assessment in the Euro-Mediterranean area. Faults considered from the EDSF are shown in Figs. 3 and 4. Last but not least, a total of 2,733 events compiled and provided within the Tsunami Risk and Strategies For the European Region (TRANSFER) Project (http://www.transferproject.eu/) have also been considered in this study.

The characteristic earthquake source database derived in this study for 0–40 and 40–100 km depth layers is a result of evaluating the compiled source databases referenced above supported by the strike/dip/rake distribution analysis and interpretation of the tectonic setting of the study region. Corresponding maps with representative focal mechanisms are given in Fig. 2. The derived database includes strike, dip, rake, depth, Mw_{max} and corresponding fault length (L), fault width (W) and slip (D) values for each bin together with associated parameters. Several parameters within the characteristic database are referenced directly from the ISC Moment Tensor

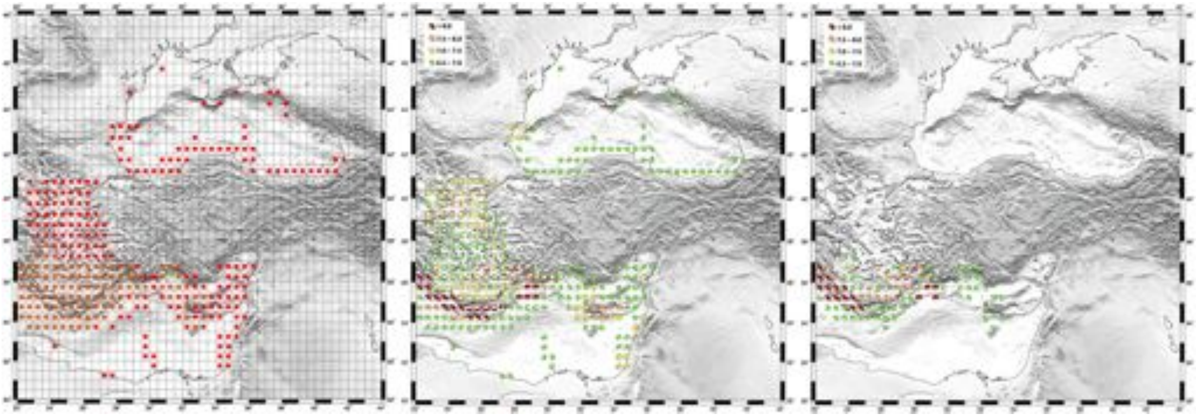

Figure 2
(*Left*) Locations of 0.5° × 0.5° bins at 0–40 km (*red squares*) and 40–100 km depth (*green squares*) layers to be used in the source characterization and corresponding tsunami scenario creation. The total number of bins is 404 (312 shallow–92 deep). *Fault lines* are taken from Basili *et al.* (2013). Representation of characteristic earthquake focal mechanism parameters for 0–40 km (*center*) and 40–100 km (*right*) depth layer provided. Beach-ball sizes are proportional to the Mw_{max} assigned to each bin

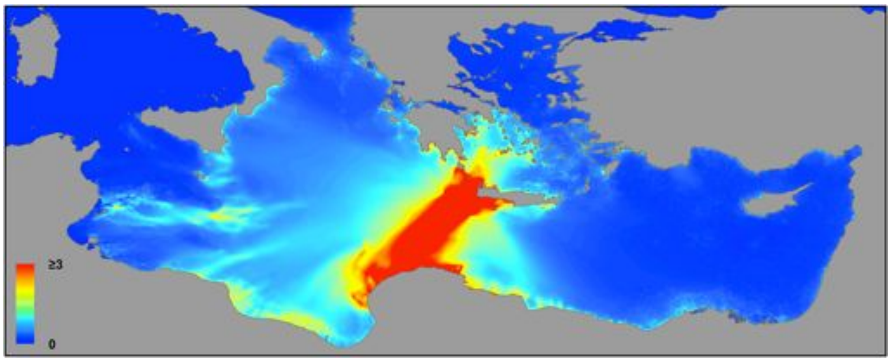

Figure 3
Maximum wave height distribution for the 365 AD event. Strong focusing between Banghazi and Darna provinces in the eastern part of the Libya is evident and a minimum offshore wave height of 1 m can be observed throughout the Eastern Mediterranean from Alexandria (Egypt) to Sicily and southern coasts of Italy

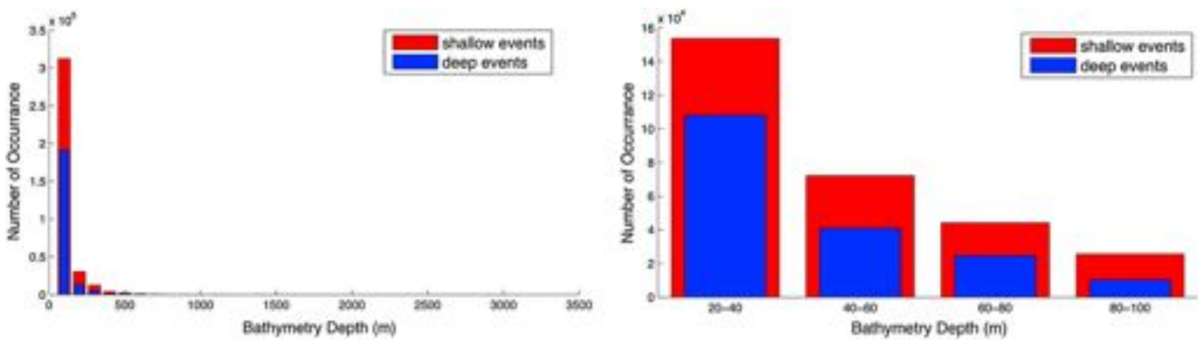

Figure 4
Distribution of calculated bathymetry depths for all depths (*left*) and for the depth range of 20–100 m (*right*). A vast majority of the calculations were performed within the 20–100 m bathymetry depth range and a high portion within this range corresponds to calculations at depths of 20–40 m. No calculations were performed in less than 20-m bathymetry depths during the coarse resolution modeling

Catalog, the EMMA Moment Tensor Catalog (Vannucci and Gasperini 2004); Kalafat *et al.* (2009), the SHARE database (Basili *et al.* 2013; Caputo *et al.* 2012), the TRANSFER database (Constantinescu *et al.* 1966; Dineva 1993; Dziewonski *et al.* 1981; Swiss Federal Institute of Technology in Zurich (ETHZ) Moment Tensor Catalogue, Radulian *et al.* 2002; Udias *et al.* 1989) and the literature (Alptekin *et al.* 1986; Beisel *et al.* 2009; Bernardi 2004; Bohnhoff *et al.* 2005; Ebeling *et al.* 2012; Eva *et al.* 1988; Jost *et al.* 2002; Koravos *et al.* 2003; Lorito *et al.* 2008; McKenzie 1978; Mitsakaki *et al.* 2013; Mitsoudis *et al.* 2012; Moratto *et al.* 2007; Okal *et al.* 2009; Papaioannou and Papazachos 2000; Papazachos 1996; Parke 2001; Pilidou *et al.* 2004; Salamon *et al.* 2003, 2007; Shaw *et al.* 2008; Shaw and Jackson 2010; Sørensen *et al.* 2012; Taymaz *et al.* 1990; Tinti *et al.* 2005; Yolsal *et al.* 2007). Further studies on moment tensor catalogues, such as Kiratzi and Louvari (2003), Pondrelli *et al.* (2002, 2004, 2011), and Benetatos *et al.* (2004) have also been considered. If not provided in the references, L, W and D values are mostly calculated from Leonard (2010) for the Mw_{max} earthquakes with strike/dip/rake parameters slightly modified; in certain cases, copied from individual studies such as Lorito *et al.* (2008), Mitsoudis *et al.* (2012) etc. or scaled from Mw-Mo relations provided in Kanamori (1977) and Hanks and Kanamori (1979). Within the range of 6.5-Mw_{max}, excluding the case corresponding to Mw_{max}, L and W parameters are scaled exponentially with respect to L and W parameters defined for an Mw 6.5 scenario in consideration of the thickness of the seismogenic layer. Slip parameters have been

Table 1

Calculation of L, W, D from a given Mw and L, D from a given Mw and W according to Leonard (2010)

	a	*b*
Mw -> L, W, D		
Mw = a × log (RA) + b		
DS	1.00	4
SS	1.00	3.99
Mw = a × log (L) + b		
DS	1.67	4.24
SS	1.67	4.17
$\log(D_{AV}) = a \times \log(L) + b$		
DS	0.833	−1.30
SS	0.833	−1.34
Mw, W -> L, D		
Mw = a × log (RA) + b		
DS	1.00	4
SS	1.00	3.99
$\log(D_{AV}) = a \times \log(L) + b$		
DS	0.833	−1.30
SS	0.833	−1.34

In the latter, W correspond to the assumed thickness of the seismogenic layer for the Mw_{max} defined. Fault classification based on the rake angle is the following: *DS* dip slip: thrust faults where $15° < \lambda < 165°$) and normal faults where $195° < \lambda < 345°$; *SS* strike slip: strike-slip faults where $345° \leq \lambda \leq 15°$ and $165° \leq \lambda \leq 195°$

inversely derived than from the moment calculated with given Mw, L, and W parameters where $\mu = 3.25E + 11$ dyn/cm^2. Reference formulas used from Leonard (2010) are given in Table 1. In cases where no Mw_{max} information was available from the literature or other sources used in this study, a hypothetical value was assigned in accordance with the Mw_{max} value defined in the neighbouring bin. Focal mechanism solutions for each bin are shown in Fig. 2 where beach-ball sizes are proportional to the Mw_{max} assigned to each bin. Using the earthquake source parameters as described above, we calculated tsunami scenarios with the SWAN-JRC code (Annunziato 2007) which solves the non-linear shallow water equations by the finite difference numerical scheme based on SWAN code by Mader (2004). Initial conditions for the tsunami modeling is obtained using an analytical solution for surface deformation in an elastic half-space (Okada 1985) embedded in the SWAN-JRC code by estimating the distribution of coseismic uplift and subsidence using the earthquake source parameters (Zamora *et al.* 2014).

5. Case Study: 365 AD Event

The earthquake of 21 July 365 AD was a significant event in the Hellenic Arc affecting a large area in the Eastern Mediterranean, where most of the associated damage was due to the seismic sea wave that played havoc with coastal settlements in Egypt, Peloponnese and Sicily (Ambraseys 2009). First, the sea was driven out and then huge masses of water flowed back; shipwrecks were found 2 km off the coast on the southwestern shore of Peloponnesus near Methoni; a tsunami was observed in Asia Minor and the coast of Sicily was flooded (Soloviev *et al.* 2000; Altınok *et al.* 2011). Papadopoulos (2011a, b) provides a detailed discussion on this event. According to Ambraseys (2009), there is evidence that this rather shallow earthquake was produced by thrust faulting off the southwest coast of Crete, which extended for about 100 km to the northwest, striking at 320°. The uplifting of the west coast of the island of Crete by 4–9 m may be associated with this or other earthquakes during that period. The seismic sea wave was caused by an offshore fault rupture, by (1) large scale landslide(s) from the bathymetric escarpments, or both. In their interpretation of the Eastern Mediterranean tectonics and tsunami hazard based on detailed investigation of the 365 AD earthquake, Shaw *et al.* (2008) presented evidence from field observations and radiocarbon data that western Crete was lifted by up to 10 m above sea level during the earthquake and suggested that the earthquake occurred on a fault dipping at around 30° within the overriding plate and not on the subduction interface. Their tsunami modelling provided open-ocean tsunami waves heights that are comparable to that of observed and modelled in the open ocean for the Sumatra 2004 tsunami. Furthermore, Lorito *et al.* (2008) argued that up to a 5-m tsunami wave could of been produced by the western Hellenic Arc source (365 AD event). The 365 AD event has been researched by many, such as Tinti *et al.* (2005); Fokaefs and Papadopoulos (2007); Papadimitriou and Karakostas (2008); Shaw and Jackson (2010); and Pararas-Carayannis (2011).

Strike, dip, rake and depth parameters (strike 315°, dip 35°, rake 90°, depth 27.3 km) of the associated earthquake source model used in the tsunami modelling for the 365 AD event in this study were assigned from Lorito *et al.* (2008) with a slight modification, whereas we considered also a Mw 8.4 event with a smaller rupture area and displacement (L 120 km, W 77 km, and slip 16.7 m). The epicenter of the source is selected as 35.25°N 23.25°E. Our modelling indicates that the tsunami reaches northeastern Libya and western Peloponnese in half an hour, whereas the arrival time for eastern Sicily, Calabria and Rhodes is 1 h. Waves arrive in Antalya, western Cyprus, Alexandria, and Tripoli in 90 min and reach the Levantine coast in 2 h. Maximum wave height distribution for the 365 AD event, shown in Fig. 3, indicates a strong focusing between the Banghazi and Darna provinces in the eastern part of Libya and a minimum of 1 m offshore wave heights can be observed throughout the Eastern Mediterranean from Alexandria (Egypt) to Sicily and southern coasts of Italy. Extreme impact is evident in western Crete, eastern Peloponnese and Attica, and in the eastern part of Libya between the Banghazi and Darna provinces. Considerable impact is evident in the southern Aegean, in central and eastern Crete, in Rhodes and Turkish coasts opposite Rhodes, on the northwestern coasts of Egypt, in northern Libya between the Tripoli and Banghazi provinces, eastern Sicily, southern Italy and in western Peloppenese. The impact is relatively low in the Levantine and almost no impact is associated with the Northern Aegean, eastern Cyprus, Tunisia, western Sicily and beyond, and Albania. The results are consistent with the historical records, indicating the reliability of the model.

6. *Evaluation of the Tsunami Scenario Database*

We present varied statistical information on the created tsunami scenario database to reflect the overall characteristics of the data, issues related to the resolution of the bathymetry used in the modeling, followed by a qualitative and quantitative assessment of the results. There are 1,394 forecast points in the scenario database where tsunami wave heights have been calculated. No calculations were performed in less than 20-m bathymetry depths in this study (Fig. 4). The distribution of the calculated wave heights with respect to the bathymetry depth of the calculation points are given in Fig. 5. The effect of the source depth is clearly visible, with a ratio close to 2 between the wave heights calculated for shallow events (top of the fault at a 5-km depth) and intermediate deep events (top of the fault at a 40-km depth). The distribution of the calculated wave heights with respect to the distance between the calculation point and associated earthquake epicentre can also be found in Fig. 5. The effect of the source depth is clearly visible where the calculated wave heights are substantially higher for shallow events qwith a source-calculation point distance in the range of 0–200 km. The relative increase observed in the wave heights between 250 and 500 km is mostly associated with the earthquakes in the Hellenic Arc and calculations points in northern Africa, especially between Banghazi (Libya) and Alexandria (Egypt). The distribution of the calculated wave heights with respect to Mw is given in Fig. 6, indicating a ratio of 2 for calculated wave heights for shallow and deep events for the Mw range of 6.5–6.6, around 1.6 for the Mw range of 6.7–7.8 and 1.2 for the Mw range of 7.9–8.5 for both sets of data.

Maximum wave heights calculated in the Black Sea for the shallow earthquakes defined in Fig. 2 are provided in Fig. 7., which shows that <3-m tsunami wave heights could be expected in locations in the southern coasts of Crimea, the northwestern coast of Turkey, the Bulgarian coast and along the southeastern coasts of Romania, whereas along the eastern Black Sea coasts, the expected maximum tsunami wave height is <1 m. The results of the modeling are in accordance with historical tsunami events in the region.

Maximum wave heights calculated in the Central and Eastern Mediterranean for shallow earthquakes defined in Fig. 2 are provided in Fig. 8 (top), which shows that the expected maximum tsunami wave height is >3 m in locations in, around and orthogonal to the Hellenic Arc, whereas for the rest of the Eastern Mediterranean, Southern Aegean, Tripoli (Libya), eastern Sicily, Calabria and western coasts Greece, the expected maximum tsunami wave height is <3 m. In the northern Aegean, Tunisia, western Sardinia, southwest coasts of Italy, and western and northern coasts of Sicily, the expected maximum

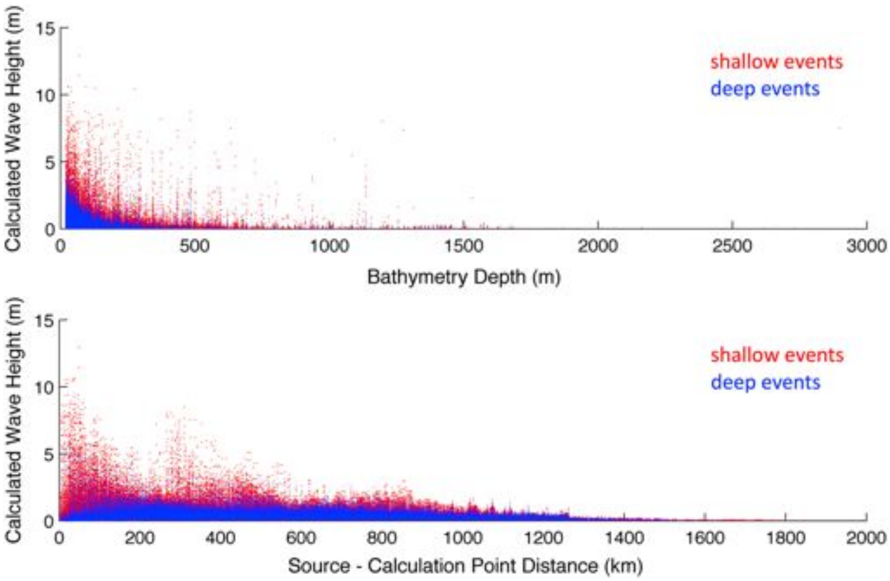

Figure 5

Top Distribution of the calculated wave heights with respect to the bathymetry depth of the calculation point. The effect of the source depth is clearly visible with a ratio close to 2 between the wave heights calculated for shallow events (*top* of the fault at a 5-km depth) and deep events (*top* of the fault at a 40-km depth). *Bottom* Distribution of the calculated wave heights with respect to the distance between the calculation point and associated earthquake epicenter. The effect of the source depth is clearly visible where the calculated wave heights are substantially higher for shallow events with a source-calculation point distance in the range of 0–200 km. The relative increase observed in the wave heights between 250 and 500 km is mostly associated with earthquakes in the Hellenic Arc and calculation points in northern Africa, especially between Banghazi (Libya) and Alexandria (Egypt)

tsunami wave height is <1 m. The results of the modeling are in accordance with the historical tsunami events in the region. It should be emphasized that the conclusions given above for both the Black Sea and Eastern Mediterranean are valid only for the shallow earthquake sources given in Fig. 2 and excluding any possibility of an associated submarine landslide. Descriptions and conclusions of tsunamis generated from shallow earthquake sources in the Eastern Mediterranean are also valid for tsunamis generated from intermediate-depth earthquake sources defined in Fig. 2 (Fig. 8 bottom).

In order to support our conclusions and avoid possible discussion associated with the definition of the maximum magnitude values considered in the study, we have decided to identify the minimum earthquake magnitude for each forecast point that would lead to 50-cm wave height at the coast line. Using Green's Law, defined as where $Aw_{1m} = (Aw_{CP})^{1/4} \times BD_{CP}$, where Aw_{1m} is the wave height at 1 m bathymetry depth, Aw_{CP} is the wave height calculated and BD_{CP} is the bathymetry depth of the calculation point, we considered all calculations where the wave height calculated offshore is higher than 20 cm; this was based on the consideration that the majority of the calculations took place in the 20–40 m bathymetry depth range and a 20 cm wave height calculated at 40 m bathymetry depth would correspond to a 50-cm wave height at the coastline according to Green's Law. On the other hand, it should be emphasized that while Green's Law provides an empirical approximation, the non-linear dynamics of the tsunami at the coastal zones may lead to deviations in actual wave heights.

Minimum values of earthquake magnitudes leading to a 50-cm wave height along the Black Sea coasts for the shallow earthquakes defined in Fig. 2 and associated earthquake magnitudes is shown in Fig. 9. While a higher magnitude Mw range of 7.5–7.9 is needed for the locations in the eastern Black Sea, an Mw range of 7.0–7.4 is sufficient enough to have 50-cm waves in most parts of the western Black Sea. Especially in the southern coasts

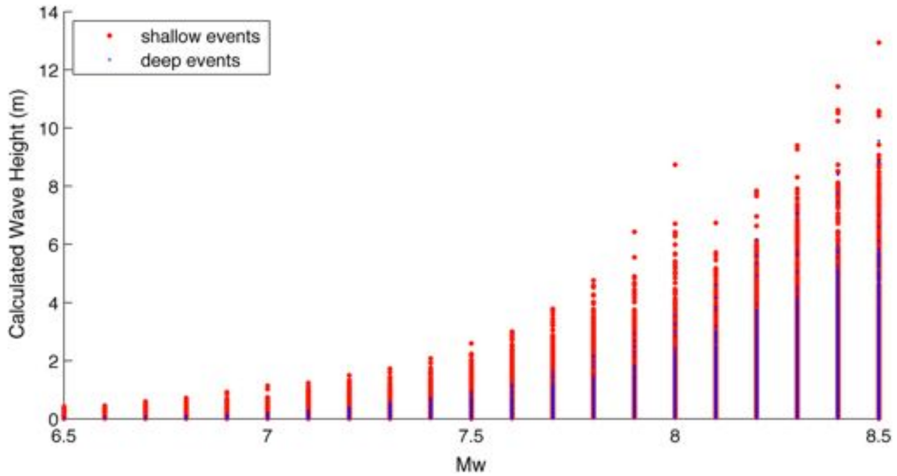

Figure 6

Distribution of the calculated wave heights with respect to Mw. the calculated mean varies around 2 for the Mw range of 6.5–6.6, around 1.6 for the Mw range of 6.7–7.8 and 1.2 for the Mw range of 7.9–8.5 for both sets of data

of Crimea, southern coasts of Romania, Bulgarian coasts and several locations in the north-western part of the Black sea region of Turkey, a Mw range of 6.5–6.9 is enough to result in 50-cm wave height at the coastline. Figure 10 shows minimum values of earthquake magnitudes leading to a 50-cm wave height on the Eastern Mediterranean and Aegean coasts for the shallow earthquakes defined in Fig. 2. Locations in an around the Hellenic Arc, the Aegean Sea and south- and eastern Cyprus can be subject to 50-cm coastal wave height for earthquakes ranging from Mw 6.5–6.9, whereas for southern coasts of Turkey, the Levantine coasts, northern Egypt and north-eastern Libya, a higher Mw range of 7.0–7.4 is needed. Earthquakes in the Mw range of 7.5–7.9 are capable of generating 50-cm coastal wave heights in northern Libya, in southern and eastern Sicily, in southern Italy, Albania and along western coasts of Greece. Only earthquakes in the Mw range of 8.0–8.5 are capable of generating a 50-cm coastal wave height in Tunisia, along western and northern Sicily, on the western and Adriatic coasts of Italy, and in the Gulf of Corinth. Minimum earthquake magnitudes leading to a 50-cm wave height at the Eastern Mediterranean and Aegean coasts for the deep earthquakes defined in Fig. 2 show that locations in an around the Hellenic Arc, the southern Aegean Sea and north-eastern Libya can be subject to 50-cm coastal wave heights for earthquakes ranging from

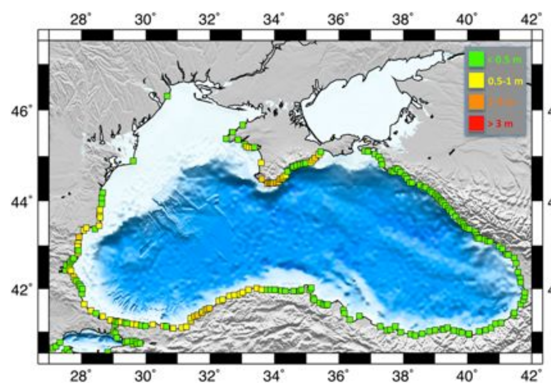

Figure 7

Maximum wave heights calculated in the Black Sea for the shallow earthquakes defined in Fig. 2 indicate that <3-m tsunami wave heights could be expected in locations along the southern coasts of Crimea, the northwestern coast of Turkey, the Bulgarian coast and the southeastern coasts of Romania, whereas along the eastern Black Sea coastline, the expected maximum tsunami wave height is <1 m. The results of the modeling are in accordance with historical tsunami events in the region. It should be emphasized that these conclusions are valid only for the earthquake sources given in Fig. 2 and excluding any possibility of an associated submarine landslide

7.0–7.4, whereas for the southern coasts of Turkey, western Cyprus, southern Levantine, northern Egypt, Tripoli (northern Libya), eastern Sicily, southern Italy, and western Greece, a higher Mw range of 7.5–7.9 is needed (Fig. 10). Only earthquakes in the Mw range of 8.0–8.5 are capable of generating 50-cm

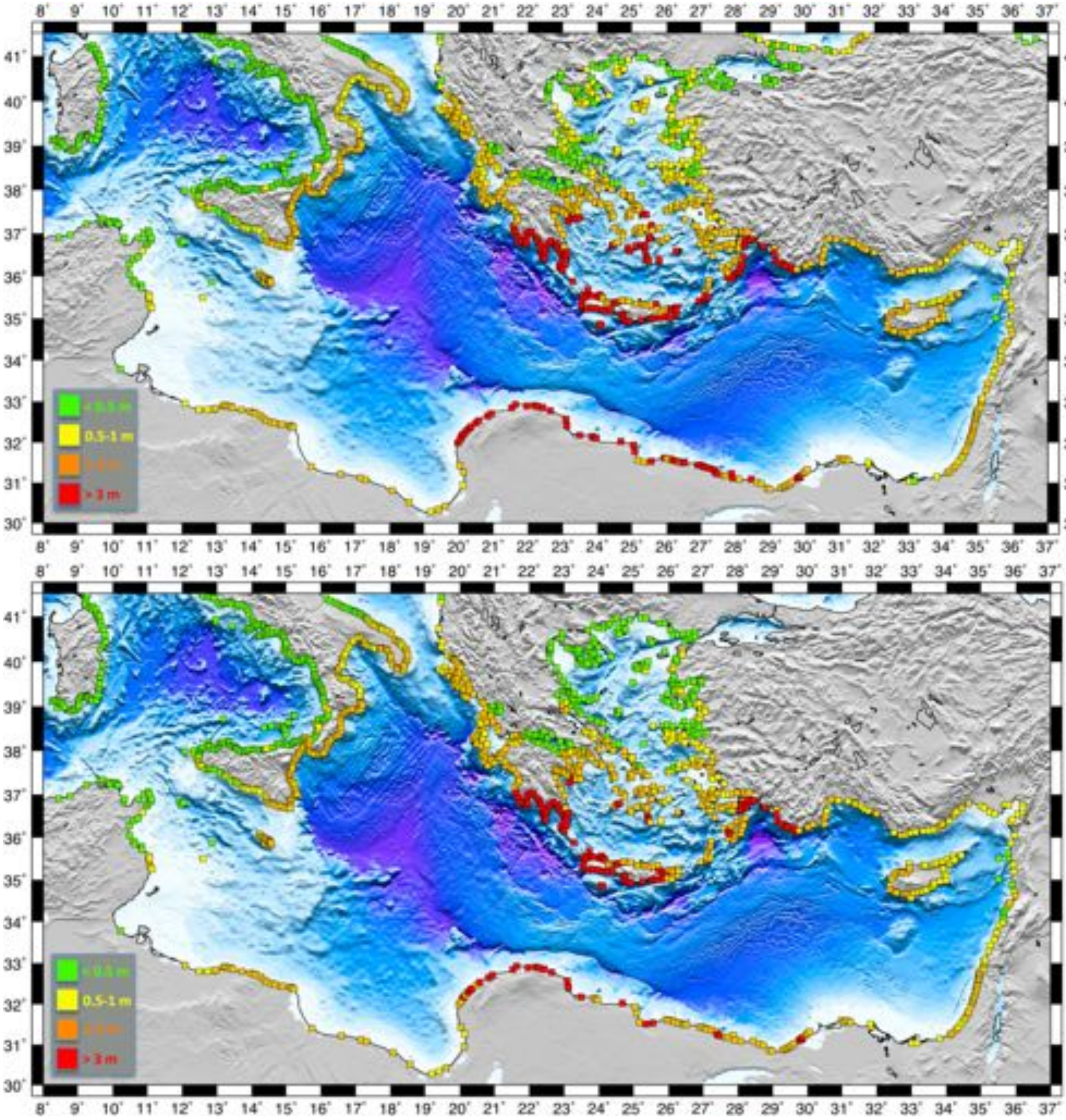

Figure 8

Maximum wave heights calculated in the Central and Eastern Mediterranean for the shallow- (*top*) and intermediate-depth (*bottom*) earthquakes defined in Fig. 2 indicate that the expected maximum tsunami wave height is >3 m in locations in, around and orthogonal to the Hellenic Arc, whereas for the rest of the Eastern Mediterranean, Southern Aegean, Tripoli (Libya), eastern Sicily, Calabria and western coasts Greece, a maximum tsunami wave height of <3 m is expected. In the northern Aegean, Tunisia, western Sardinia, southwest coasts of Italy, and western and northern coasts of Sicily, the expected maximum tsunami wave height is <1 m. The results of the modeling are in accordance with the historical tsunami events in the region. It should be emphasized that these conclusions are valid only for the earthquake sources given in Fig. 2 and excluding any possibility of an associated submarine landslide

coastal wave heights in Tunisia, western and northern Sicily, along the western and Adriatic coasts of Italy, in the Gulf of Corinth, in the central and northern Aegean, in eastern Cyprus and along the northern Levantine coasts. It should be emphasized that these conclusions are valid only for the shallow earthquake

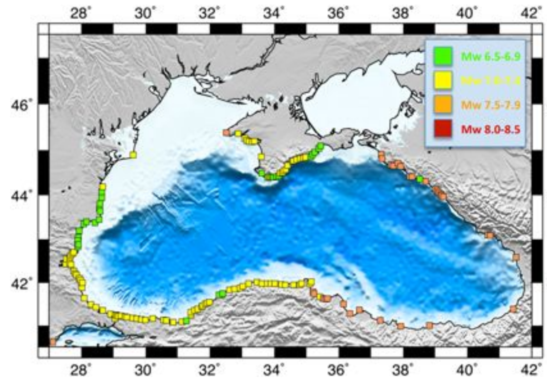

Figure 9
Minimum earthquake magnitude values leading to 50-cm coastal wave heights along the Black Sea coast for the shallow earthquakes defined in Fig. 2, and associated earthquake magnitudes. While a higher magnitude Mw range of 7.5–7.9 is needed for the locations in the eastern Black Sea, an Mw range of 7.0–7.4 is sufficient enough to have 50-cm waves in most parts of the western Black Sea. Especially in the southern coasts of Crimea, southern coasts of Romania, Bulgarian coasts and several locations in the northwestern part of the Black sea region of Turkey, a Mw range of 6.5–6.9 is enough to result in 50-cm wave heights at the coastline. It should be emphasized that these conclusions are valid only for the shallow earthquake sources given in Fig. 2 and excluding any possibility of an associated submarine landslide

sources given in Fig. 2 and excluding any possibility of an associated submarine landslide.

7. *Discussion and Conclusions*

There are various strong tsunami events in the Eastern Mediterranean with an apparent recurrence period of about 150–200 years associated to both seismic and non-seismic origins (Yolsal *et al.* 2007). But more importantly, some extreme events, such as those occurring in 365 and 1303 AD, have resulted in basin-wide impacts, as also confirmed by the tsunami simulations performed in this study. The low recurrence of strong events in the Black Sea makes it difficult to conduct a preliminary tsunami hazard study in the region since there is only a certain amount of descriptive information concerning the historical tsunami events in the Black Sea. The most important fact is that the available historical data indicates that some historical tsunami waves were equal to 2–3 m and, thus, destructive (Dotsenko and Ingerov 2007). In this study, we have tried to consider all possible locations of tectonic origin tsunamis with a possible and meaningful range of magnitudes. However, submarine landslide-generated tsunamis in the Black Sea constitute a major element of the tsunami hazard in the region and further comprehensive studies on this should be initiated. The importance of landslides in terms of tsunami hazard following a large earthquake should be an important element of tsunami hazard analysis for the Eastern Mediterranean, as in the case of the 1956 Amorgos earthquake and tsunami (Okal *et al.* 2009).

Maximum wave heights calculated in the Black Sea for the shallow earthquakes defined in Fig. 2 indicate that <3-m tsunami wave heights could be expected along the southern coasts of Crimea, the northwestern coast of Turkey, the Bulgarian coast and the southeastern coasts of Romania, whereas along the eastern Black Sea coast, the expected maximum tsunami wave height is <1 m. A corresponding simplified maximum tsunami wave height zonation map is given Fig. 11. Minimum Mw values that may lead to 50-cm coastal wave height is in the range of 7.0–7.4 for the most part of the western Black Sea, whereas a higher magnitude Mw range of 7.5–7.9 is needed for the locations in the eastern Black Sea. Maximum wave height calculated for the Central and Eastern Mediterranean for the shallow earthquakes defined in Fig. 2 indicate that the expected maximum tsunami wave height is >3 m in locations in, around and orthogonal to the Hellenic Arc. In the rest of the Eastern Mediterranean, Southern Aegean, Tripoli (Libya), eastern Sicily, Calabria and western coasts Greece, the expected maximum tsunami wave height is <3 m. In the northern Aegean, Tunisia, western Sardinia, southwest coasts of Italy, and western and northern coasts of Sicily, the expected maximum tsunami wave height is <1 m. A corresponding simplified maximum tsunami wave height zonation map is given Fig. 12. Minimum Mw values that may possibly lead to 50-cm wave coastal wave height is in the range of 6.5–6.9 in locations in an around the Hellenic Arc, the Aegean Sea and south- and eastern Cyprus, whereas for southern coasts of Turkey, the Levantine coasts, northern Egypt and north-eastern Libya, a higher Mw range of 7.0–7.4 is needed. Earthquakes in the Mw range of 7.5–7.9 are capable of generating

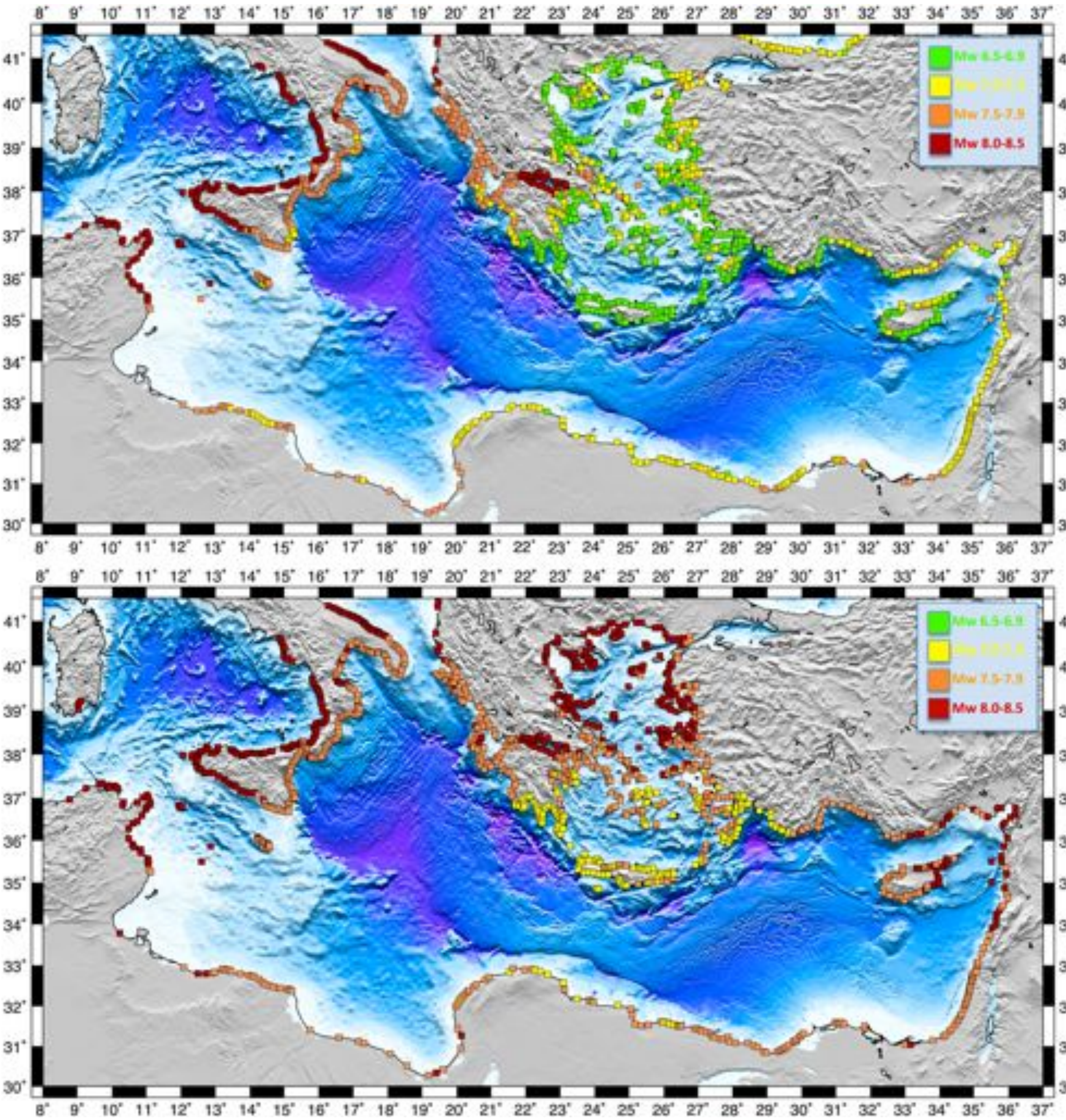

Figure 10

Minimum earthquake magnitude values leading to 50-cm coastal wave heights along the Eastern Mediterranean and Aegean coasts for the shallow- (*top*) and intermediate-depth (*bottom*) earthquakes defined in Fig. 2, and associated earthquake magnitudes. Locations in an around the Hellenic Arc, the Aegean Sea and south- and eastern Cyprus can be subject to 50-cm coastal wave heights for shallow earthquakes ranging from 6.5–6.9 and from 7.0–7.4 for intermediate-depth earthquakes. For the southern coasts of Turkey, ther Levantine coasts, northern Egypt and north-eastern Libya, a higher Mw range of 7.0–7.4 for shallow and 7.5–7.9 for the intermediate-depth earthquakes is needed. Shallow earthquakes in the Mw range of 7.5–7.9 are capable of generating a 50-cm coastal wave height in northern Libya, southern and eastern Sicily, southern Italy, Albania and along the western coasts of Greece. Only earthquakes in the Mw range of 8.0–8.5 are capable of generating 50-cm coastal wave height in Tunisia, in western and northern Sicily, at the western and Adriatic coasts of Italy, and in the Gulf of Corinth. It should be emphasized that these conclusions are valid only for the shallow earthquake sources given in Fig. 2 and excluding any possibility of an associated submarine landslide

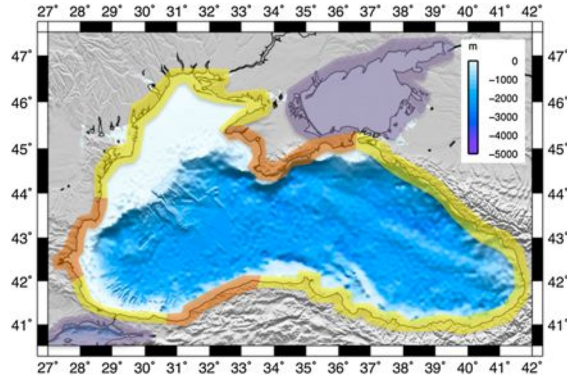

Figure 11
Simplified maximum tsunami wave height zonation map for the Black Sea derived from this study. *Colors* indicate the level of maximum tsunami wave height at the coastline of the respective zone (*orange* 1–3 m; *yellow* <1 m) due to earthquake sources given in Fig. 2 and excluding any possibly associated submarine landslide; source regions indicated by magenta on the map

50-cm coastal wave height in northern Libya, in southern and eastern Sicily, in southern Italy, Albania and along the western coast of Greece. Only earthquakes in the Mw range of 8.0–8.5 are capable of generating 50-cm coastal wave height in Tunisia, in western and northern Sicily, along the western and Adriatic coasts of Italy, and in the Gulf of Corinth. The results of the modeling are in accordance with the historical tsunami events in the study area. It should be emphasized that these conclusions should not be considered as complete for the areas shown in the maps since they are valid only for the earthquake sources given in Fig. 2 and excluding any possibility of an associated submarine landslide. On the other hand, minimum values of earthquake magnitudes leading to a 50-cm coastal wave height in the study area helps us to conclude that, when excluding secondary phenomenon such as a triggered submarine landslide, an Mw value of 6.5 could be accepted as a lower threshold for a tsunami early warning system in the region.

The first element of disaster risk reduction is assessment of the hazard. The main purpose of this study is to provide a basis for detailed tsunami hazard studies in Eastern Mediterranean, Aegean and Black Seas. Historical and instrumental studies reveal the complex nature of plate interactions and crustal deformation in the region, interactions that are mainly

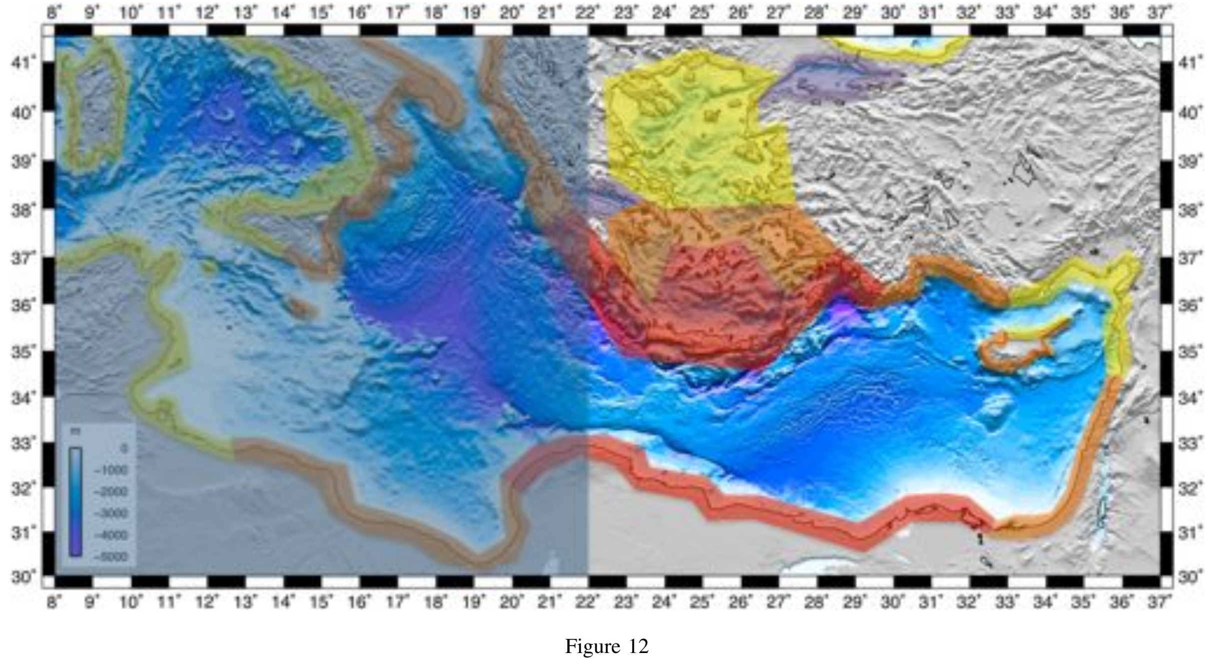

Figure 12
Simplified maximum tsunami wave height zonation map for the Central-Eastern Mediterranean and Aegean Sea derived from this study. *Colors* indicate the level of the maximum tsunami wave height at the coastlines of the respective zones (*red* >3 m; *orange* 1–3 m; *yellow* <1 m) due to earthquake sources given in Fig. 2 and excluding any possibly associated submarine landslide; earthquake source regions indicated by magenta on the map. Only offshore earthquake sources within 22°E–37°E are considered in this study, as shown in Fig. 2; thus, conclusions for the western part of the study area could be considered less reliable

evidenced by devastating earthquakes sometimes accompanied by catastrophic tsunamis. In addition to earthquakes as tsunami sources, massive land movements, such as in the case of the Santorini event around 1600 BC or the Fatsa Tsunami triggered by the Erzincan (Turkey) earthquake in 1939, gives a clear indication that the entire Eastern Mediterranean and its connected seas region is prone to tsunami events. A 365 AD-type earthquake could be expected approximately every 800 years and the fact that there has been only one other such event (in 1303) in the past 1,650 years, the modern-day tsunami hazard in the Eastern Mediterranean requires more attention (Shaw *et al.* 2008). Therefore, it is evident that a comprehensive tsunami hazard analysis is needed covering the Eastern Mediterranean, Aegean and Black Seas, since future tsunamis in the region could be even more damaging than past events, when considering increased population density and economic activity in the coastal zones, such as ports, shipyards, marinas, nuclear and thermoelectric power plants, oil refineries and coastal airports. In addition, the increased technological and organizational complexities of modern societies accompanied by a limitation of resources require both short- and long-term hazard assessment as an integrated element of sustainable development. Alpar (2009) showed that the relative rise in sea-level calculated for Antalya is in the range of 2.6–4.3 mm/yr, which should not put the terrain bordering the Mediterranean in danger; however, the margins of deltaic plains in the region may be prone to inundation and local submergence, and storm surges will accelerate the vulnerability. This estimated sea-level rise could also mean that a 25-cm tsunami wave height would equate to twice the impact 50 years from now on. Therefore, long-term tsunami risk assessment studies should definitely consider the added effect of sea-level rise.

Acknowledgments

We would like to thank the European Commission's Joint Research Centre (EC-JRC), in particular Alessandro Annunziato, for his support during the realization of the modeling database, which was possible through a collaborative agreement between the Kandilli Observatory and Earthquake Research Institute (KOERI) and EC-JRC. We would like to especially thank Roberto Basili [The Istituto Nazionale di Geofisica e Vulcanologia (INGV)] and Doğan Kalafat (KOERI) for their supports providing the SHARE active faults and seismogenic sources and KOERI Moment Tensor databases, respectively. We would also like to thank Prof. Ahmet Cevdet Yalciner for providing the earthquake source database compiled in TRANSFER Project (http://www.transferproject.eu/) and for his feedback throughout the study. We would like to thank Dr. Ceren Özer Sözdinler for her feedback and support in the quality control of the tsunami scenario database. We also would like thank Mustafa Comoglu from KOERI for his assisstance in IT-related issues concerning the tsunami scenario database and to Dr. Mehmet Yılmazer for his support in the creation of the TTT maps. Last but not least, we would like to express our sincere gratitude to two anonymous reviewers who considerably helped us in improving the manuscript. Maps are produced with Generic Mapping Tools (GMT; Wessel *et al.* 2013) and ArcMap 10 by Esri.

References

Aksu, A. E., Hall, J., Yaltırak, C. 2005, *Miocene to Recent tectonic evolution of the eastern Mediterranean: New pieces of the old Mediterranean puzzle*, Marine Geology *221*, 1–13.

Alpar, B., 2009, "*Vulnerability of Turkish Coasts to Accelerated Sea-Level Rise*", Geomorphology, *107*(2009) 58–63.

Alptekin, Ö., J. L. Nábalek, and N. Toksöz, 1986, "*Source mechanism of the Bartin earthquake of September 3, 1968 in northwestern Turkey: Evidence for active thrust faulting at the southern Black Sea margin*", Tectonophysics, Vol. *122*, Issues 1–2, Pages 73–88.

Altinok, Y., B. Alpar, N. Ozer, and C. Gazioglu, 2005, "*1881 and 1949 earthquakes at the Chios-Cesme Strait (Aegean Sea) and their relation to tsunamis*", Natural Hazards and Earth System Sciences, *5*, 717–725.

Altinok, Y., Alpar, B., Özer, N., and Aykurt, H. (2011), *Revision of the tsunami catalogue affecting Turkish coasts and surrounding regions*, Nat. hazards Earth Syst. Sci., *11*, 273–293.

Ambraseys, N. 2009. Earthquakes in the Mediterranean and Middle East, Cambridge University Press, ISBN 978-0-521-87292-8.

Ambraseys, N. N. and Synolakis C., 2010, "*Tsunami Catalogues for the Eastern Mediterranean*", *Revisited*, Journal of Earthquake Engineering, *14*, 3, 309–330.

Annunziato, A. (2007). *The Tsunami Assessment Modelling System by the Joint Research Centre*. Science of Tsunami Hazards *26*:2, 70–92.

BARKA, A., REILINGER, R., 1997. *Active Tectonics of the eastern Mediterranean region: deduced from GPS, neotectonic and seismicity data*. Annali di Geofisica *XL* (3), 586–608.

BASILI, R. TIBERTI, M. M, KASTELIC, V., ROMANO, F., PIATANESI, A., SELVA, J. and LORITO, S. (2013). *Integrating geologic fault data into tsunami hazard studies*; Nat. Hazards Earth Syst. Sci., *13*, 1025–1050.

BAYRAK, Y. and BAYRAK, E. (2011), *An Evaluation of Earthquake Hazard Potential for Different Regions in Western Anatolia Using the Historical and Instrumental Earthquake Data*, Pure Appl. Geophys., Volume *169*, Issue 10, pp 1859–1873.

BEISEL S., L. CHUBAROV, I. DIDENKULOVA, E. KIT, A. LEVIN, E. PELINOVSKY, Y. SHOKIN, and M. SLADKEVICH, 2009, "*The 1956 Greek tsunami recorded at Yafo, Israel, and its numerical modeling*", Journal of Geophysical Research, vol. *114*.

BEN-AVRAHAM Z, GARFUNKEL Z, LAZAR M (2008) *Geology and evolution of the southern Dead Sea fault with emphasis on subsurface structure*. Annu Rev Earth Planet Sci *36*:357–387.

BENETATOS C., A. KIRATZI, C. PAPAZACHOS, G. KARAKAISIS, 2004, "*Focal mechanisms of shallow and intermediate depth earthquakes along the Hellenic arc*", Journal of Geodynamics, *37*, 253–296.

BERNARDI F. (2004) Earthquake source parameters in the Alpine-Mediterranean region from surface wave analysis, Diss. ETH Nr. 15652, Ph.D. Thesis.

BIJU-DUVAL, B.; LETOUZEY, J. and MONTADERT, L., 1978. Structure and evolution of the Mediterranean basins. In: HSUE, K. and MONTADERT *et al*. (Editors), Initial Report of the Deep Sea Drillin project, Vol. *42*, Part 1, pp. 951–984.

BOHNHOFF, M. HARJES, H-P and MEIER, T. (2005) *Deformation and stress regimes in the Hellenic subduction zone from focal Mechanisms* Journal of Seismology (2005) *9*: 341–366.

CAPUTO R., C. ALEXANDROS, P. SPYROS, S. SOTIRIS, (2012), "*The Greek Database of Seismogenic Sources (GreDaSS): state-of-the-art for northern Greece*", Annals of Geophysics, *55*, 5.

CONSTANTINESCU, L., RUPRECHTOVA, L. and ENESO, D., 1966. *Mediterranean-Alpine earthquake mechanisms and their seismotectonic implications*. Geophys. J.R. Astron. Soc., *10*: 347–368.

CIESM (2011). Marine geo-hazards in the Mediterranean. N° 42 in CIESMWorkshop Monographs [F. BRIAND Ed.], 192 pages, Monaco.

DELIBASIS, N., ZIAZIA, M., VOULGARIS, N., PAPADOPOULOS, T., STAVRAKAKIS, G., PAPANASTASSIOU, D., DRAKATOS, G. (1999), *Microseismic activity and seismotectonics of Heraklion Area* (*central Crete Island, Greece*), Tectonophysics *308*, 237–248.

DEWEY, J. F., PITMAN, W. C., RYAN, W. B. F. & BONNIN, J., 1973. "*Plate tectonics and the evolution of the Alpine system*", Geological Society of America Bulletin, *84*:3137–3180.

DINEVA S. (1993) *Catalogue of Earthquakes in Bulgaria, 1981–1990*, Bulg. Acad. Sci., Geophys. Inst., Seismol. Dep., 39 pp.

DOMINEY-HOWES, D. T. M., G. S. HUMPHREYS, and P. P. HESSE, 2006, "*Tsunami and palaeotsunami depositional signatures and their potential value in understanding the late-Holocene tsunami record*", The Holocene, vol. *16*, 1095. doi:10.1177/0959683606069400.

DOTSENKO, S. F. and KONOVALOV, A. V. (1996). *Tsunami waves in the Black Sea in 1927: observations and numerical modeling* (*in Thermohydrodynamics of the Ocean*) Phys. Oceanogr.,Vol. *7*, No. 6, pp. 389–401 (1996).

DOTSENKO, S. F. and A. V. INGEROV, 2007, "*Characteristics of Tsunami Waves In The Black Sea According to the Data of Measurements*", Physical Oceanography, Vol. *17*, No. 1.

DOTSENKO, S. F. and A. V. INGEROV, 2010, "*Numerical Modeling Of The Propagation And Strengthening Of Tsunami Waves Near The Crimean Peninsula And The Northeast Coast Of The Black Sea*", Physical Oceanography, Vol. *20*, No. 1, 2010.

DZIEWONSKI, A. M., CHOU T. A. and J. H. WOODHOUSE. (1981) *Determination of earthquake source parameters from waveform data for studies of global and regional seismicity*. J. Geophys. Res., *86*, 2825–2852 and subsequent quarterly papers on Phys. Earth Planet. Int.

EBELING, C. W., OKAL, E., KALLIGERIS, N., SYNOLAKIS, C. E. (2012) *Modern seismological reassessment and tsunami simulation of historical Hellenic Arc earthquakes*; Tectonophysics *530–531*, 225–239.

EVA C., RIUSCETTI M. and D. SLEJKO. (1988) *Seismicity of the Black Sea Region*, Boll. Geof. Teor. Appl., *XXX*, 117–118, 53–66.

EYIDOĞAN, H., J. A. JACKSON. (1985), "*A seismological study of normal faulting in the Demirci, Alasehir and Gediz earthquakes of 1969–70 in western Turkey: implications for the nature and geometry of deformation in the continental crust*", Geophysical Journal of the Royal Astronomical Society, *81*, 569–607.

FOKAEFS, A. and PAPADOPOULOS, G. A. (2007). *Tsunami hazard in the Eastern Mediterranean: strong earthquakes and tsunamis in Cyprus and the Levantine Sea*. Natural Hazards *40*:503–526.

GANAS, A. and T. PARSONS, 2009, "*Three-dimensional model of Hellenic Arc deformation and origin of the Cretan uplift*", Journal of Geophysical Research, vol. *114*.

GARFUNKEL, Z., 2004. *Origin of the Eastern Mediterranean basin: a reevaluation*. Tectonophysics *391*, 11–34.

Gorur, N. (1997) Crateceous syn- to postrift sedimantation on the Southern Continental Margin of the Western Black Sea Basin, in Regional and Petroleum Geology of the Black Sea and Surrounding Region, edited by A. G. ROBIN- SON, American Association of Petroleum Geologists (AAPG), AAPG Memoir 68, pp. 227–240.

HALL, J., AKSU, A., YALTıRAK, C., WINSOR, J., 2009. *Structural architecture of the Rhodes Basin: a deep depocentre that evolved since the Pliocene at the junction of the Hellenic and Cyprus arcs, eastern Mediterranean*. Marine Geology *258*, 1–23.

HANKS, T. C. and KANAMORI, H. (1979). *A moment magnitude scale* Journal of Geophysical Research: Solid Earth, Volume *84*, Issue B5, pages 2348–2350.

HATZFELD, D., BESNARD, M., MAKROPOULOS, K. and HATZIDIMITRIOU, P. (1993), *Microearthquake seismicity and fault-plane solutions in the southern Aegean and its geodynamic implications*, Geophys. J. Int. *115*, 799–818.

HEURET, A., S. LALLEMAND, F. FUNICIELLO, C. PIROMALLO, and C. FACCENNA (2011), *Physical characteristics of subduction interface type seismogenic zones revisited*, Geochem. Geophys. Geosyst., Volume *12*, Issue 1, January 2011.

HOWE, T. M. and P. BIRD, 2010, "*Exploratory models of long-term crustal flow and resulting seismicity across the Alpine-Aegean orogen*", Tectonics, vol. *29*, 4.

HYNDMAN, R. D., YAMANO, M. & OLESKEVICH, D. A., 1997. *The seismogenic zone of subduction thrust faults*, Island Arcs, *6*, 244–260.

JOLIVET, L. FACCENNA, C., HUET, B., LABROUSSE, L., LE POURHIET, L., LACOMBE, O., LECOMTE, E., BUROV, E., DENÈLE, Y., BRUN, J-P., PHILIPPON, M., PAUL, A., SALAÜN, G., KARABULUT, H., PIROMALLO, C., Monié, P., Gueydan, F., Okay, A., Oberhänsli, R., Pourteau, A., Augier, R., Gadenne, L., Driussiü, O. (2013), *Aegean tectonics: Strain localisation, slab tearing and trench retreat*, Tectonophysics 597–598, 1–33.

Jost, M. L., O. Knabenbauer, J. Cheng, H-P. Harjes, 2002, "*Fault plane solutions of microearthquakes and small events in the Hellenic arc*", Tectonophysics, *356*, 87–114.

Kalafat, K., Kekovali, K., Gunes, Y., Yilmazer, M., Kara, M., Deniz, P., Berberoglu, M. (2009). A catalogue of Source Parameters of Moderate and Strong Earthquakes for Turkey and its Surrounding Area (1938–2008), Bogazici University Press, ISBN 978-975-518-303-9.

Kanamori, H. (1977) *The energy release in great earthquakes*, Journal of Geophysical Research:Solid Earth and Planets, Volume *82*, Issue 20, pages 2981–2987.

Karabulut, H., Z. Roumelioti, C. Benetatos, A.K. Mutlu, S. Özalaybey, M. Aktar and A. Kiratzi, 2006, "*A source study of the 6 July 2003 (Mw 5.7) earthquake sequence in the Gulf of Saros (northern Aegean Sea): Seismological evi- dence for the western continuation of the Ganos fault*", Tectonophysics, *412*, 195–216.

Kiratzi, A. A. and C. B. Papazachos. 1995. *Active Deformation of the Shallow Part of the Subducting Lithospheric Slab in the Southern Aegean*. J. Geodyn. *19*, 65–78.

Kiratzi, A., E. Louvari, 2003, "*Focal mechanisms of shallow earthquakes in the Aegean Sea and the surrounding lands determined by waveform modelling: a new database*", Journal of Geodynamics, *36*, 251–274.

Koravos, G. Ch., I. G. Main, T. M. Tsapanos and R. M. W. Musson, 2003, "*Maximum earthquake magnitudes in the Aegean area constrained by tectonic moment release rates*", Geophysical Journal International, *152*, 94–112.

Kreemer, C. and N. Chamot-Rooke, 2004, "*Contemporary kinematics of the southern Aegean and the Mediterranean Ridge*", Geophysical Journal International, *157*, 1377–1392.

Le Pichon, X. and J. Angelier, 1979. *The Hellenic Arc and Trench system: A Key to the Neotectonic Evolution of the Eastern Mediterranean Area*. Tectonophysics, *60*, 1–42.

Leonard, M., 2010, "*Earthquake Fault Scaling: Self-Consistent Relating of Rupture Length, Width, Average Displacement, and Moment Release*", Bulletin of the Seismological Society of America, Vol. *100*, No. 5A, pp. 1971–1988.

Lorito, S., Tiberti, M. M., Basili, R., Piatanesi, A. and Valensise, G. (2008). *Earthquake-generated tsunamis in the Mediterranean Sea: Scenarios of potential threats to Southern Italy*; Journal of Geophysical Research, Vol. *113*, B01301.

Løvholt, F., S. Glimsdal, C. B. Harbitz, N. Zamora, F. Nadim, P. Peduzzi, H. Dao, H. Smebye, 2012, "*Tsunami hazard and exposure on the global scale*", Earth-Science Reviews, *110*, 58–73.

Mader, C. L. (2004). Numerical Modeling of Water Waves, CRC Press; 2nd edition, ISBN 0-8493-2311-8.

McClusky, S., S. Balassanian, A. Barka, C. Demir, S. Ergintav, I. Georgiev, O. Gürkan, M. Hamburger, K. Hurst, H. Kahle, K. Kastens, G. Kekelidze, R. King, V. Kotzev, O. Lenk, S. Mahmoud, A. Mishin, M. Nadariya, A. Ouzounis, D. Paradissis, Y. Peter, M. Prilepin, R. Reilinger, I. Şanli, H. Seeger, A. Tealeb, M.N. Toksöz and G. Veis. 2000. *Global Positioning System Constraints on Plate Kinematics and Dynamics in the Eastern Mediterranean and Caucasus*. Journal of Geophysical Research, *105*, 5695–5719.

McClusky, S., R. Reilinger, S. Mahmoud, D. Ben-Sari and A. Tealeb, 2003, "*GPS constraints on Africa (Nubia) and Arabia plate motions*", Geophysical Journal International, *155*, 126–138.

McKenzie, D. P. (1970). *Plate Tectonics of the Mediterranean Region*. Nature *226*, 239–243.

McKenzie, D. P., (1972), "*Active tectonics of the Mediterranean region*", Geophys. J. R. Ast. Soc. *30*, 109–185.

McKenzie, D. P., (1978), "*Active tectonics of the Alpine–Himalayan belt: the Aegean Sea and surrounding regions*", Geophysical Journal of the Royal Astronomical Society, *55*, 217–254.

Meier, T., Becker, D., Endrun, B., Rische, M., Bohnhoff, M., Stöckhert, B. and Harjes, H.-P. (2007) *A model for the Hellenic subduction zone in the area of Crete based on seismological investigations*, Geological Society, London, Special Publications 2007, v. *291*; pp. 183–199.

Mitsakaki, C., M. G. Sakellariou, D. Tsinas, 2013, "*A study of the crust stress field for the Aegean region* (*Greece*)", Tectonophysics, Vol. *597–598*, 50–72.

Mitsoudis, D. A., E. T. Flour, N. Chrysoulakis, Y. Kamarianakis, E. A. Okal, C. E. Synolakis, 2012, "*Tsunami hazard in the southeast Aegean Sea*", Coastal Engineering, *60*, 136–148.

Moratto, L., B. Orlecka-Sikora, G. Costa, P. Suhadolc, Ch. Papaioannou, C. B. Papazachos, 2007, "*A deterministic seismic hazard analysis for shallow earthquakes in Greece*", Tectonophysics, *442*, 66–82.

Necmioğlu, Ö. and Özel., N. M. (2014). *An Earthquake Source Sensitivity Analysis for Tsunami Propagation in the Eastern Mediterranean*. Oceanography *27*(2): 76–85.

Nikishin, A. M., Korotaev, M. V., Ershov, A. V., Brunet, M-F. (2003). *The Black Sea basin: tectonic history and Neogene–Quaternary rapid subsidence modelling*, Sedimentary Geology *156*,149–168.

Okada, Y., 1985, "*Surface Deformation due to Shear and Tensile Faults in a Half-Space*", Bulletin of the Seismological Society of America, *75*, 1135–1154.

Okal, E. A., C. E. Synolakis, B. Uslu, N. Kalligeris and E. Voukouvalas, 2009, "*The 1956 earthquake and tsunami in Amorgos, Greece*", Geophysical Journal International, *178*, 1533–1554.

Ozel, M. N., Necmioglu, O., Yalciner, A.C., Kalafat, D., Mustafa, E. (2011). *Tsunami hazard in the Eastern Mediterranean and its connected seas: Toward a Tsunami warning center in Turkey*, Soil Dynamics and Earthquake Engineering, Volume *31*, Issue 4, April 2011, Pages 598–610.

Papadimitriou, E. E., and Karakostas, V. G. (2008) *Rupture model of the great AD 365 Crete earthquake in the southwestern part of the Hellenic Arc*; Acta Geophysica, Volume *56*, Issue 2, pp. 293–312.

Papadopoulos, G. (2011), The Seismic History of Crete, Ocelatos Publications, ISBN 978-960-9499-68-2.

Papadopoulos, G. A., G. Diakogianni, A. Fokaefs, and B. Ranguelov, 2011, "*Tsunami hazard in the Black Sea and the Azov Sea: a new tsunami catalogue*", Natural Hazards Earth System Science, *11*, 945–963.

Papadopoulos, G. A, Gràcia, E., Urgeles, R., Sallares, V., De Martini, P. M., Pantosti, D., M. González, Yalciner, A. C., Mascle, J., Sakellariou, D., Salamon, A., Tinti, S., Karastathis, V., Fokaefs, A., Camerlenghi, A., Novikova, T., Papageorgiou, A. (2014). *Historical and pre-historical tsunamis in the Mediterranean and its connected seas: Geological* *signatures, generation mechanisms and coastal impacts*. Marine Geology *354* (2014) 81–109.

Papaioannou, Ch. A. and B. C. Papazachos, 2000, "*Time-Independent and Time-Dependent Seismic Hazard in Greece Based on Seismogenic Sources*, Bulletin of the Seismological Society of America, *90*, 1, 22–33.

Papazachos, B. C., 1990. *Seismicity of the Aegean and surrounding area*. Tectonophysics *178*, 287–308.

Papazachos, B. C., Ch. Koutitas, P. M. Hatzidimitriou, B. M., Karakostas and C. A. Papaioannou, 1986, "*Tsunami hazard in Greece and the surrounding area*", Annales Geophysicae, *4*, 79–90.

Papazachos, B. C., 1996, "*Large Seismic Faults in the Hellenic Arc*", Annali di Geofisica, Vol. *XXXIX*, No.5.

Papazachos, B., A. Kiratzi, E. Paradimitriou, 1991, "*Regional focal mechanism for earthquakes in the Aegean area*", Pure Applied Geophysics, *4*, 405–419.

Papazachos, B. C. and Papaioannou, Ch. A. 1993. *Long-term earthquake prediction in the Aegean area based on a time and magnitude predictable model*. Pageoph, *140*, 593–612, 1993.

Papazachos, B. C. and Ch. A. Papaioannou, 1999, "*Lithospheric boundaries and plate motions in the Cyprus area*", Tectonophysics, *308*, 193–204.

Pararas-Carayannis, G. (2011). *The earthquake and tsunami of July 21, 365 AD in the Eastern Mediterranean Sea – A review of Impact on the Ancient World – Assessment of Recurrence and Future Impact*. Science of Tsunami Hazards, Vol. *30*, No. 4, page 253.

Parke, G., (2001), Active Tectonics and Sedimentary Process in Western Turkey, Ph.D. Dissertation, University of Cambridge.

Pilidou, S., Priestley, K., Jackson, J., and Maggi, A. (2004). *The 1996 Cyprus earthquake: a large, deep event in the Cyprean Arc*. Geophys. J. Int. *158*, 85–97.

Pondrelli,S., Morelli, A., Ekström, G. (2004). *European-Mediterranean regional centroid-moment tensor catalog: solutions for years 2001 and 2002*. Physics of the Earth and Planetary Interiors *145*, 127–147.

Pondrelli, S., Salimbenia, S., Morelli, A., Ekström, G., Postpischl, L., Vannucci, G., Boschi, E. (2011) *European–Mediterranean Regional Centroid Moment Tensor catalog: Solutions for 2005–2008*, Physics of the Earth and Planetary Interiors *185* (2011) 74–81.

Pondrelli, S., Morelli, A., Ekström, G., Mazza, S., Boschi, E., Dziewonski, A.M. (2002) *European–Mediterranean regional centroid-moment tensors: 1997–2000*, Physics of the Earth and Planetary Interiors *130*, 71–101.

Radulian M., Popescu E., Bala A. and A. (2002) Utale *Catalog of fault plane solutions for the earthquakes occurred on the Romanian territory*, Rom. Journ. Phys., *47*, 663–685.

Ranguelov, B. and D. Gospodinov, 1994, "*Seismic activity after the earthquake of 31 March, 1901 in the Shabla-Kaliakra zone (in Bulgarian)*", Bulgarian Geophysical Journal, *20*, 44–49.

Rastsvetaev, L. M., 1987. Tectono-dynamical environments of the Great Caucasus Alpine structure origin. In: Milanovsky, E. E., Koronovsky, N. V. (Eds.), Geology and Mineral Resources of the Great Caucasus. Nauka, Moscow, pp. 69–96. in Russian.

Reilinger, R. E., McClusky, S. C., Oral, M. B., King, R. W., Toksoz, M. N., Barka, A. A., Kinik, I., Lenk, O., Sanli, I. (1997). *Global positioning system measurements of present-day crustal move- ments in the Arabia – Africa – Eurasia plate collision zone*. Journal of Geophysical Research *102* (B5), 9983–9999.

Reilinger, R., McClusky, S., Vernant, P., Lawrence, S., Ergintav, S., Cakmak, R., Ozener, H., Kadirov, F. Guliev, I., Stepanyan, R., Nadariya, M., Hahubia, G., Mahmoud,S., Sakr,K., ArRajehi, A., Paradissis, D., Al-Aydrus, A., Prilepin, M., Guseva, T., Evren,E., Dmitrotsa, A., Filikov, S. V., Gomez, F., Al-Ghazzi,R., and Karam, G. (2006), *GPS constraints on continental deformation in the Africa-Arabia- Eurasia continental collision zone and implications for the dynamics of plate interactions*, Journal of Geophysical Research, Vol. *111*, B05411.

Reilinger, R., McClusky, S., Paradissis, D., Ergintav, S., Vernant, P. (2010), *Geodetic constraints on the tectonic evolution of the Aegean region and strain accumulation along the Hellenic subduction zone*, Tectonophysics *488*, 22–30.

Robertson, A. H. F., Dixon, J. E., 1984. *Introduction: aspects of the geological evolution of the Eastern Mediterranean, Geological Evolution of the Eastern Mediterranean*. Geol. Soc. Spec. Publ. London, vol. *17*, pp. 1–74.

Robertson, A. H. F. and Mountrakis, D. (2006) *Tectonic development of the Eastern Mediterranean region: an introduction*, Geological Society, London, Special Publications 2006; v. *260*; p. 1–9.

Saatçilar, R., Ergintav, S., Demirbağ, E., Inan, S. (1999), *Character of active faulting in the North Aegean Sea*, Marine Geology 160, 339–353.

Salamon, A., A. Hofstetter, Z. Garfunkel, and H. Ron, 2003, "*Seismotectonics of the Sinai subplate: the Eastern Mediterranean region*", Geophysical Journal International, *155*, 149–173.

Salamon, A., Rockwell, T., Ward, S. N., Guidoboni, E., and Comastri, A., 2007, *Tsunami hazard evaluation of the Eastern Mediterranean: Historical analysis and selected modeling*: Seismological Society of America Bulletin, v. *97*, p. 705–724.

Saleh, S. (2013), *3D Crustal and Lithospheric Structures in the Southeastern Mediterranean and Northeastern Egypt*, Pure Appl. Geophys. *170*, 2037–2074.

Satake, K. 2011. *Unforecasted Earthquake and Forgotten Tsunamis: Lessons from 2011 Tohoku Event*. American Geophysical Union, Fall Meeting 2011, Abstract #NH12A-05.

Sboras, S., Pavlides, S., Caputo, R., Chatzipetros, A., Michailidou, A., Valkaniotis., A. and Papathanasiou, G. (2011). Improving resolution of seismic hazard estimates for critical facilities: The Database of Greek Crustal Seismogenic Sources in the Frame of the SHARE Project. Proceedings of the 30° Convegno Nazionale GNGTS, 14–17 November, 2011, Trieste, Extended Abstracts, 232–235.

Scholz, C. H., 1998. *Earthquakes and friction laws*. Nature, *391*, 37–42.

Shaw, B., Ambraseys, N. N., England, P. C., Floyd, M. A., Gorman, G. J, Higham, T. F. G., Jackson, J. A., Nocquet, J.-M., Pain, C. C., and Piggott, M. D. (2008). *Eastern Mediterranean tectonics and tsunami hazard inferred from the AD 365 earthquake*; Nature Geoscience Vol. *1* APRIL 2008.

Shaw, B. and Jackson, J. (2010). *Earthquake mechanisms and active tectonics of the Hellenic subduction zone*. Geophysical Journal International *181*, 966–984.

Showstack, R. (2014). *Fukushima Nuclear Accident Report Calls for More Focus on Threats From Extreme Events*. Eos, Vol. *95*, No. 31.

Snopek, K., Meier, T., Endrun, B., Bohnhoff, M., Casten, U. (2007), *Comparison of gravimetric and seismic constraints on the structure of the Aegean lithosphere in the forearc of the*

Hellenic subduction zone in the area of Crete, Journal of Geodynamics.

SOLOVIEV, S. L., 1990, "*Tsunamigenic zones in the Mediterranean sea*", Natural Hazards, *3*, 183–202.

SOLOVIEV, S. L., SOLOVIEVA, O. N., GO, C. N., KIM, K. S., SHCHETNIKOV, N. A. (2000). Tsunamis in the Mediterranean Sea – 2000 B.C.–2000 A.D., Kluwer Academic Publishers, 237 pp.

SØRENSEN, M.B., M. SPADA, A. BABEYKO, S. WIEMER and G. GRÜNTHAL, 2012, "*Probabilistic tsunami hazard in the Mediterranean Sea*", Journal of Geophysical Research, vol. *117*, B01305.

STAMPFLI, G. M., BOREL, G. D., 2002. *A plate tectonic model for the Paleozoic and Mesozoic constrained by dynamic plate boundaries and restored synthetic ocean isochrons*. Earth Planet. Sci. Lett. *196*, 17–33.

STEIN, S., GELLER, R.J., LIU, M. 2012. *Why Earthquake Hazard Maps Often Fail and What to do About it?* Tectonophysics *562–563* (2012) 1–25.

STERN, R. J., 2002. *Subduction zones*, Rev. Geophys., *40*, 3–1.

STROBL, M., R. HETZELA, C. FASSOULAS and P. W. KUBIK, 2014, *A Long-Term Rock Uplift Rate for Eastern Crete and Geodynamic Implications for the Hellenic Subduction Zone*, Journal of Geodynamics, *78* (2014) 21–31.

ŞENGÖR, A. M. C., N. GÖRÜR, F. SAROĞLU, 1985, Strike–slip faulting and related basin formation in zones of tectonic escape: Turkey as a case study, In: K. T. BIDDLE, N. CHRISTIE-BLICK (Eds.), Strike – slip Deformation, Basin Formation and Sedimentation, Society of Economic Paleontologists and Mineralogists Special Publication, 37, 227–264.

TARI, E. SAHIN, M., BARKA, A., REILINGER, R., KING, R.W., MCCLUSKY, S., PRILEPIN, M. (2000) *Active tectonics of the Black Sea with GPS*, Earth Planets Space, *52*, 747–751.

TAYMAZ, T., J. A. JACKSON and R. WESTAWAY, 1990, "*Earthquake mechanisms in the Hellenic trench near Create*", Geophysical Journal International, 102, 695–731.

TAYMAZ, T., J. A. JACKSON and D. MCKENZIE, 1991, "*Active tectonics of the north and central Aegean Sea*", Geophysical Journal International, *106*, 433–490.

TINTI, S., A. ARMIGLIATO, G. PAGNONI, and F. ZANIBONI. (2005). *Scenarios of giant tsunamis of tectonic origin in the Mediterranean*, ISET J. Earthquake Technol., *42*, 171–188.

TINTI, S., ARMIGLIATO, A., PAGNONI, G., ZANIBONI, F. and TONINI, R. (2011). Tsunamis in the Euro-Mediterranean region: emergency and long term counter measures. In CIESM, 2011. Marine geohazards in the Mediterranean. N° 42 in CIESMWorkshop Monographs [F. BRIAND Ed.], 192 pages, Monaco.

UDIAS A., BUFORN E. and J. RUIZ DE GAUNA (1989). Catalogue of Focal Mechanisms of European Earthquakes. Department of Geophysics, Universidad Complutense, Madrid.

VANNUCCI, G. and GASPERINI, P. (2004). *The new release of the database of Earthquake Mechanisms of the Mediterranean Area* (*EMMA Version 2*), Annals of Geophysics, Supplement to V. *47*, N.1, 307–334.

VOLVOVSKY, B. S., 1989. Seismicity. In: BELOUSSOV, V. V., VOLVOVSKY, B. S. (Eds.), Structure and Evolution of the Earth's Crust and Upper Mantle of the Black Sea. Nauka, Moscow, pp. 95–97. in Russian.

WESSEL, P., W. H. F. SMITH, R. SCHARROO, J. F. LUIS, and F. WOBBE, *Generic Mapping Tools: Improved version released*, EOS Trans. AGU, *94*, 409–410, 2013.

YALÇINER, A. C., PELINOVSKY, E., TALIPOVA, T., KURKIN, A., KOZELKOV, A. & ZAITSEV, A. 2004. *Tsunami in the Black Sea: comparison of the historical, instrumental and numerical data*. Journal of Geophysical Research, *109*, C12023, doi:10.1029/2003JC002113.

YOLSAL, S., T. TAYMAZ and A. C. YALCINER, 2007, "*Understanding tsunamis, potential source regions and tsunami-prone mechanisms in the Eastern Mediterranean*", Geological Society,.

YOLSAL-ÇEVIKBILEN, S. and T. TAYMAZ, 2012, "*Earthquake Source Parameters Along the Hellenic Subduction Zone and Numerical Simulations of Historical Tsunamis in the Eastern Mediterranean*", Tectonophysics, *536–537*, 61–100.

London, Special Publications, *291*, 201–230.

ZAMORA, N., FRANCHELLO, G., and ANUNZIATO, A. (2014). *Validation of the JRC Tsunami Propagation and Inundation Codes*; Science of Tsunami Hazards, Volume *33*, Number 2, Pages 112–132.

(Received September 5, 2014, revised March 7, 2015, accepted March 12, 2015)